# Recent advances in preparation methods and thermophysical properties of oil-based nanofluids

*A state-of-the-art review*

Asadi, Amin; Aberoumand, Sadegh; Moradikazerouni, Alireza; Pourfattah, Farzad; Zyla, Gawel; Estelle, Patrice; Mahian, Omid; Wongwises, Somchai; Nguyen, Hoang Minh ; Arabkoohsar, Ahmad

*Published in:*
Powder Technology

*DOI (link to publication from Publisher):*
10.1016/j.powtec.2019.04.054



*Publication date:*
2019

*Document Version*
Accepted author manuscript, peer reviewed version

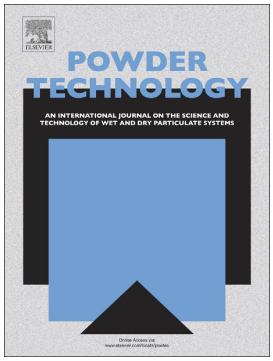


# Recent advances in preparation methods and thermophysical properties of oil-based nanofluids: A state-of-the-art review

Amin Asadi, Sadegh Aberoumand, Alireza Moradikazerouni, Farzad Pourfattah, Gaweł Żyła, Patrice Estellé, Omid Mahian, Somchai Wongwises, Hoang M. Nguyen, Ahmad Arabkoohsar

PII: S0032-5910(19)30302-X
DOI: https://doi.org/10.1016/j.powtec.2019.04.054
Reference: PTEC 14286

To appear in: *Powder Technology*

Received date: 21 January 2019
Revised date: 12 April 2019
Accepted date: 22 April 2019

Please cite this article as: A. Asadi, S. Aberoumand, A. Moradikazerouni, et al., Recent advances in preparation methods and thermophysical properties of oil-based nanofluids: A state-of-the-art review, Powder Technology, https://doi.org/10.1016/j.powtec.2019.04.054

# Recent advances in preparation methods and thermophysical properties of oil-based nanofluids: A state-of-the-art review

Amin Asadi[1,*] Ams@et.aau.dk, Sadegh Aberoumand[2], Alireza Moradikazerouni[3], Farzad Pourfattah[4], Gaweł Żyła[5], Patrice Estellé[6], Omid Mahian[7], Somchai Wongwises[8], Hoang M. Nguyen[9,10,*] nguyenminhhoang1@tdtu.edu.vn, Ahmad Arabkoohsar[1]

[1]Department of Energy Technology, Aalborg University, Aalborg, Denmark

[2]Independent Researcher, Tehran, Iran

[3]Department of Mechanical Engineering, Marvdasht Branch, Islamic Azad University, Marvdasht, Iran

[4]Department of Mechanical Engineering, University of Kashan, Kashan, Iran

[5]Department of Physics and Medical Engineering, Rzeszów University of Technology, Rzeszów, Poland

[6]Materials and Thermo-Rheology team at LGCGM, Université Rennes 1, Rennes, France

[7]School of Chemical Engineering and Technology, Xi'an Jiaotong University, Xi'an, China

[8]Fluid Mechanics, Thermal Engineering and Multiphase Flow Research Laboratory(FUTURE Lab.), Department of Mechanical Engineering, Faculty of Engineering, King Mongkut's University of Technology Thonburi, Bangmod, Bangkok 10140, Thailand

[9]Division of Computational Physics, Institute for Computational Science, Ton Duc Thang University,Ho Chi Minh City,Vietnam

[10]Faculty of Electrical and Electronics Engineering, Ton Duc Thang University, Ho Chi Minh City, Vietnam

[*]Corresponding authors.

## Abstract

Thermal oils due to their high ability in cooling and lubricating have many applications in high-tech industries such as the automotive industry. Dispersing nanoparticles in a thermal oil (which the resulted new liquid is called nanofluid) can modify further the cooling and lubrication efficiencies. This review paper aims to present the recent advances in the preparation methods and thermophysical properties measurements of oil-based nanofluids. Effects of various parameters such as nanoparticle concentration, size, and temperature on the values of properties including thermal conductivity, viscosity, density, and specific heat are reviewed. The correlations available for the properties of oil-based nanofluids are gathered from the literature that could be a worthy source for those who aim to work on oil-based nanofluids.

**Keywords:** Oil-based nanofluid; Preparation method; Thermophysical properties; Viscosity; Density; Thermal conductivity; Specific heat capacity.

**Nomenclature**

$\boldsymbol{\tau}$: Shear stress (Pa)
$\boldsymbol{\mu}$: Dynamic viscosity (cP)
$\dot{\gamma}$: Shear rate ($s^{-1}$)
**T**: Temperature (°C)
$\boldsymbol{\varphi}$: Solid concentration (%)
$\mathcal{V}$ : Kinematic viscosity ($m^2/s$)
**k**: Thermal conductivity (W/m K)
**d**: particle diameter (nm)
**ρ**: Density ($kg/m^3$)
$\mathbf{C_p}$: Specific heat capacity (J/kg K)

**Indexes:**

**eff**: Effective
**bf**: Base fluid
**nf**: Nanofluid
**P**: Particle
**np**: Nanoparticle

## 1- Introduction

Nanofluid (NF), a cutting-edge liquid with superior thermal conductivity compared to common liquids, are absolutely a well-known keyword in thermal sciences. The greater thermal conductivity of NFs makes them as an appropriate candidate for efficiency enhancement of thermal equipment, although at the same time the increase in viscosity which happens due to adding nanoparticles (NPs) to the base fluid (BF) could be a negative aspect of the NF application. NFs are applied to solar energy devices [1], [2], car radiators [3], [4], microchannel heat sinks [5], [6], medicine [7], different cavities [8], [9], and so forth.

Prior to employing NFs in different applications, it is necessary to estimate the thermophysical properties to achieve a better design of the target system. However, available theoretical models in the literature failed to predict the properties with a high accuracy. Therefore, measurement of NFs properties is inevitable, especially at high concentrations of particles. Although the number of research and review papers on the NF properties exceeds hundreds, however, for the given NFs (oil-based NFs), some discrepancies in the literature can be observed on the effect of nanoparticles' morphology and NF temperature and concentration on the thermophysical properties (mainly thermal conductivity and viscosity). These inconsistencies would be because of different preparation and measurement techniques used by researchers.

The present paper focuses on the preparation methods and thermophysical properties of oil-based NFs. There are plenty of good reasons on why the oil-based NFs are the focus of the present review; First of all, there are a few review articles that focus on the properties and characteristics of oil-based NFs despite numerous review articles on the other types of NFs; Nadooshan et al. [10] reviewed the effective parameters of rheological behavior of different nanofluids; Hafiz et al. [11] presented a review on different preparation methods of nanofluids containing $TiO_2$ nanoparticles; Sajid et al. [12] reviewed the advances of nanofluids in heat transfer applications; Mahian et al. [13] reviewed the contribution of nanofluids in solar energy; Babar et al. [14] presented a critical review on the viscosity of hybrid nanofluids; Chamkha et al. [15] reviewed the application of nanofluids in different microchannels; and there are some other reviews [16]–[19]. Another point would be that, from the practical point of view, oil-based NFs can be used in many applications in different industries in which water-based NFs are not applicable; such as automobile industry where the NF is used for engine cooling or lubrication of other components and solar based systems [20]–[23]. Thus, in the present review, various preparation techniques, which is the most important step toward studying the NFs' thermal efficiency, will be presented and reviewed. Then, the published

experimental literature on dynamic viscosity, thermal conductivity, density, and specific heat capacity of different oil-based NFs will be discussed and a collection of available correlations on properties will be presented.

## 2- Nanofluid preparation

It is known that the first and most important step toward experimentally studying different NFs is the preparation step. Two major techniques have been widely used by researchers to prepare a long-time stable (at least 10 days) oil-based NFs; single/one-step method, which is preferred for small-scale production, and two-step method, which is suitable for mass production due to its low production cost [24].

### 2-1- Single/One-step method

Preparing NFs from NPs and BF directly and simultaneously can be defined as the one-step preparation method. Due to the fact that this approach can prevent NPs oxidation, such method is not only favorable but also many relevant researchers have been using this approach to prepare their NFs. Furthermore, several characteristics of one-step prepared NFs such as dryness, storing, transportation and dispersion of NPs can lead to decrease aggregation and clustering to improve the stability [25].

Some techniques such as laser ablation (Fig. 1A) [26] and submerged arc NPs synthesis system (SANSS) (Fig. 1B) [27] are available for preparing stable one-step NFs. During such processes, metals will be vaporized and then cooled into liquid for preparing stable NFs. Moreover, submerged are NPs synthesis system (SANSS) includes a heat source, cooling system, and a state control system which consists of isobaric and isothermal control systems. Using this method can also prevent forming undesired aggregation [27]. In fact, for managing thermal systems, it is essential to have stable working fluid either prepared by two-step or one-step.

Therefore, several techniques have been used by the researchers to prepare and stabilize their applied NFs. For instance, direct fabrication approach [28]–[31], sol-gel technique [32], chemical precipitation process [33], physical gas-phase and direct condensation technique [26], [34], [35], mechanical stirring method [36], surface treated and functionalization acid process for Carbon nanotube [37], [38], chemical co-precipitation approach [39], and electrical explosion of wire [40], [41]. To reduce agglomeration of NPs and improve stability, some of the above mention methods employ dispersant such as SDBS [42]–[45], Chitosan [46], using surfactant such as Polyvinylpyrrolidone [25], Cetyl Trimethyl Ammonium Bromide (CTAB) [47], and some scholars

have employed other alternatives to obtain uniform mixture using surface modifier such as silane [48], spiral coil [27], varying of pH of NFs [37], and creation of carboxyl groups on the surface of the NPs [39] for stability purpose.

Using single-step method, Electrical Explosion of Wire (EEW), Aberoumand and Jafarimoghaddam [41] synthesized the Cu/engine oil NF in different solid weight concentrations (0.2, 0.5, and 1 %). In this method (EEW), employing the extra high electric voltage and current leads to converting the primary wire into NPs through under liquid wire explosion process. Consequently, they produced long-time stable NFs with the average nanoparticle size of 50 nm.

### 2-2- Two-step method

In this method, the nano-sized particles, which are usually nanotubes or NPs, that can be formed by physical, chemical or mechanical processes as dry powders [1]. Then, an ultrasonic device would be used for mixing and stirring the nano-sized powders within the BF. Ultrasonication process can decrease the particle aggregation, which is one of the challenges in NFs preparation process. Moreover, dispersants would be added to enhance the stability of the NFs. Another feature of the two-step method is that such preparation method is very suitable for large scale of NFs production. It must be noted that the two-step preparation method is the most economical approach for preparing any NFs. Fig. 2 presents schematic view of the NF preparation process.

Literature shows that the two-step method is the dominant method in preparing the oil-based NFs compared to the single-step method as shown by the Tab. 1 that presents a summary of the preparation methods used by researchers to produce oil-based NFs.

Employing the two-step method, Saeedinia et al. [49] dispersed CuO (50 nm, purity 99 %) NPs into oil in four different weight concentrations of 0.2, 0.5, 1, and 2 %. They used an ultrasonic processor (400 W, 24 kHz) to break down the possible agglomeration of NPs into the BF. They observed no sedimentation over the first 24 hours of the preparation with the naked eyes. However, the sedimentation has been observed after a week of preparation.

The MWCNT nanoparticle has been dispersed into heat transfer oil using the two-step method by Pakdaman et al. [50] They dispersed the NPs in three weight concentrations of 0.1, 0.2, and 0.4 % without using any surfactant. First of all, employing an electrical blender for 1 h, the MWCNT has been dispersed into the BF. Then, the suspension has been subjected to an ultrasonic processor (400 W, 24 kHz) for 6 hours. They used the ultrasonic processor to break down the agglomeration of NPs. The literature shows that using the ultrasonic processor is an inevitable part of preparing the

NFs in the two-step method and different researchers proof that it helps to break down the agglomeration of NPs and make a long-time stable NF with uniform particle distribution [51]–[53].

Wang et al. [54] employed the two-step method to prepare graphite-oil NF into four weight concentrations of 0.5, 1, 2, and 4 %. They used a ball grinder (KQM-X4, China) to fabricate the NF. It must be noted that they produced the samples with and without using any surfactants and declared that the samples containing surfactant showed better stability.

In another study, Ahmadi et al. [55] investigated the effect of different preparation method, ultrasonic bath, ultrasonic probe, and the ball-mill method, on the quality of the NF. They dispersed MWCNT nanoparticle with 0.1 wt. % into the oil. They observed that bath and probe sonication method is not that much effective to break down the agglomeration of MWCNT particles compared to the ball-mill method.

The Silicon Carbide (SiC) and Titanium Oxide ($TiO_2$) NPs have been dispersed into the diathermic oil applying two-step method by Wei et al. [56]. They added the hybrid NPs into the BF in three different concentrations of 0.2, 0.4, and 0.8 vol. %. They investigated the stability of the produced samples through sedimentation experiments and zeta potential measurements and observed that the produced samples have good stability even after 10 days. Fig. 3 presents the results of the zeta potential as a function of time and the sedimentation experiments.

Asadi and Asadi [57] dispersed the hybrid NPs of ZnO and MWCNT into a four seasonal engine oil (10W40) employing the two-step method. They used the ZnO and MWCNT with the ratio of 85 % and 15 % and dispersed them into the engine oil in five concentrations of 0.125, 0.25, 0.5, 0.75, and 1 %. In the first step, a magnetic stirrer has been employed for 2 h to mix the NPs into the BF. Then, to make a uniform and long-time stable NF and breaking down the possible agglomeration of the NPs, an ultrasonic processor (1200 W, 20kHz, Topsonic, Iran) has been used for 1 h. They reported that employing the two-step method, NF stability is achieved for at least one week and the naked eyes have evidenced no sedimentation.

## 3- Viscosity

Studying the rheological properties of NFs, it is of paramount importance to categorize whether the NF is a Newtonian or non-Newtonian fluid. There are many debated whether a NF is a Newtonian or non-Newtonian fluid; especially in the case of oil-based NF, Alirezaei et al. [58] reported that the MWCNT-ZnO/engine oil NF showed non-Newtonian behavior over the range of the studied

temperatures (25-50 ℃) and concentrations (0.625-1 %) and various shear rates (670-8700 $s^{-1}$) while for the same NF, Asadi et al. [57] reported that the MWCNT-ZnO/engine oil hybrid NF showed Newtonian behavior over the studied temperatures and concentrations. In the following sections, the Newtonian and non-Newtonian behavior will be discussed, and the related literature will be reviewed.

### 3-1- Newtonian Behavior

The Newtonian fluid behavior was described for the first time by Sir Issac Newton (1642-1726). He described the Newtonian fluid with a simple linear relation between shear stress (mPa) and shear rate (1/s) as follows:

$$\tau = \mu \times \dot{\gamma} \tag{1}$$

Where $\boldsymbol{\tau}$, $\boldsymbol{\mu}$, and $\dot{\gamma}$ are shear stress, viscosity, and shear rate, respectively. It must be noted that the viscosity of the Newtonian fluid is temperature-dependent. Moreover, there is a linear increase in shear stress with increasing the shear rates, and the slope of this increase is given by the viscosity of the fluid. Thus the viscosity of the Newtonian fluid will keep constant regardless of its velocity to flow through a pipe or a channel. Water, mineral oil, gasoline, and alcohol are just some of the examples of Newtonian fluids widely used for the preparation of NFs. Fig. 4 presents the qualitative flow behavior for different types of fluids; Newtonian and non-Newtonian.

The rheological properties of CuO (50 nm)-oil NF has been experimentally investigated by Saeedinia et al. [49]. They performed the experiments in different solid fractions (0.2-2 wt. %) and temperatures (20-70 ℃). They reported that the prepared samples exhibited Newtonian behavior over the studied range of temperatures and concentrations.

Pakdaman et al. [50] conducted an experimental investigation on the rheological behavior of MWCNT/heat transfer oil in three different concentrations of 0.1, 0.2, and 0.4 wt. % and at different temperatures (40-100 ℃). They reported that there is a linear relationship between the shear stress and shear rate of the studied NF, which proves that the studied NFs are Newtonian.

In another experimental study, the rheological properties of CuO/engine oil (20W50) over a different range of concentrations (0.2-6 wt. %) and temperatures (5-70 ℃) by Farbod et al. [59]. They used CuO NPs, nano-rhombic, and nano-rod to prepare the samples. They reported that the

studied NF with all the particle shapes as well as the BF (engine oil) showed Newtonian behavior over the studied range of temperatures and concentrations.

Dardan et al. [60] studied the effect of adding $Al_2O_3$-MWCNT NPs into the engine oil (SAE40) on the rheological behavior of the resultant hybrid NF. They used the $Al_2O_3$ and MWCNT NPs by the ratio of 75 vol. % and 25 vol. % in six different solid fractions (0.0625 % to 1 %). Moreover, they conducted the experiments over the different temperatures ranging from 25 ℃ to 50 ℃ and share rates ranging from 1333 $s^{-1}$ to 13,333 $s^{-1}$. They reported that the viscosity of both the BF (SAE 40) and the prepared samples of NFs showed independent behavior from the shear rate at all the studied temperature and concentrations. Thus both of them are Newtonian fluids.

Asadi et al. [61] investigated the effects of adding MgO (80 vol%) and MWCNT (20 vol%) on the rheological properties of a hybrid engine oil-based (SAE50) NF. The mean diameter of the NPs was 30 nm, and they have conducted the experiments over different concentrations (0.25- 2 %) and temperatures (25-50 ℃). They reported that the prepared hybrid NF showed Newtonian behavior over the studied range of temperatures and solid concentration. A summary of the studied NF which showed Newtonian behavior is presented in Tab. 2.

In another experimental study, Aberoumand et al. [40] studied the rheological properties of Ag-heat transfer oil NF over different temperatures ranging from 25 to 60 ℃ and three concentrations of 0.12, 0.36, and 0.72 wt. %. Their results were quite interesting; they reported that while the BF showed Newtonian behavior, the prepared NF showed non-Newtonian behavior at the temperatures lower than 35 ℃. However, at the temperatures higher than 35 ℃, the prepared NF showed Newtonian behavior.

### 3-2 Non-Newtonian behavior

Another type of fluids, which their flow curves are nonlinear or even their flow curves are linear, but it does not pass through the origin, called non-Newtonian fluids. In other words, the viscosity of non-Newtonian fluids depends on the flow conditions; shear rate/stress developed within the fluid, flow geometry, time of shearing, the initial state of dispersion, stability, and so forth. Moreover, the viscosity of the non-Newtonian fluids is temperature-independent. The non-Newtonian fluids can be categorized into two different categories:

**3-2-1- Time-independent fluids:** the fluid properties of this category are independent of the duration of shearing, which can be described as follows [62]:

$$\tau_{yx} = f(\dot{\gamma}_{yx})$$

or; (1)

$$\dot{\gamma}_{yx} = f(\tau_{yx})$$

Based on the form of the Eq. 2, the time-independent fluids can be categorized into three different types as follows:

**A. Shear-thinning or pseudoplastic fluids:** in this types, increasing the shear rate leads to decreasing the viscosity of the fluid. Fig. 5 clearly presents the shear-thinning or pseudoplastic behavior. There are some mathematical models to describe the pseudoplastic behavior, but the power-law model is the more widely used ones among others. The Eyring model, the Cross model, the Carreau viscosity, and the Ellis fluid model [62] can also be suitable. The power-law expression is as follows:

$$\tau_{yx} = m(\dot{\gamma}_{yx})^{n}$$

$$or;$$

$$\mu = m(\left|\dot{\gamma}_{yx}\right|)^{n-1} \quad (2)$$

**A.** Where ***n*** and ***m*** are the power-law index and the fluid consistency coefficient, respectively. It is known that for the Newtonian fluid, $n$=1 while for the pseudoplastic $n$<1. It must be mentioned that the lower value of ***n*** means the greater the degree of pseudoplastic [62].

**B. Shear-thickening or dilatant fluids:** This types of fluids are the opposite of the shear-thinning; the viscosity of the fluids increases as the shear rate increases. The shear-thickening behavior is shown in Fig. 5.

**C. Visco-Plastic fluids:** This types of fluids are categorized by the existence of the yield stress ($\tau_0$). This yield stress should be exceeded before the fluid starts to flows.

**3-2-2- Time-dependent fluids:** There are some fluids which their apparent viscosity, apart from the applied shear rate, is also a function of shearing time. This type of fluids can be divided into two different categories:

A. **Thixotropic fluids:** The apparent viscosity of this types of fluids decreases with time at a constant shear rate. By gradually increasing the applied shear rate at a certain rate and then decreasing the shear rate at the same rate, a hysteresis loop will be obtained [62], as presented in Fig. 3**.**
B. **Rheopectic fluids:** Compared to the thixotropic fluids, the rheopectic fluids showed inverse behavior; at a constant shear rate, the apparent viscosity increases with time [62]. In this type of fluids, the hysteresis loop in the flow curve is inversely observed (Fig. 6).

Hemmat Esfe et al. [63] studied the rheological behavior of MWCNT-$SiO_2$/oil (SAE40) hybrid NF in different temperatures (25 to 50 ℃) and concentrations (0.625 to 2 vol. %). They conducted the experiments over different shear rates ranging from 100 to 500 RPM and observed that at solid volume fractions up to 1 %, the studied NF exhibited Newtonian behavior, however, in higher concentrations ($\varphi$> 1 %), the studied NF behaved as non-Newtonian fluid (Fig. 7).

In another experimental investigation, the rheological behavior of alumina-silicon oil NF at four different concentrations of 2, 4, 6, and 8 wt. % and shear rates ranging from 5 to 1000 $s^{-1}$ was studied by Anoop et al. [64]. They performed the experiments at room temperature and observed that both the BF and the NF showed Newtonian behavior at the shear rates up to 102 $s^{-1}$, but at higher shear rates, the NF showed non-Newtonian shear-thinning behavior.

The effect of adding surfactant on the rheological properties of $Al_2O_3$-diathermic oil NF was studied by Colangelo et al. [65]. They conducted the experiments over three different concentrations of 0.3, 0.7, and 1 vol. % and reported that the sample without using surfactant at the solid concentration of 1 % and the samples without surfactant and the concentrations of 0.7 and 1 % showed non-Newtonian behavior. Tab. 3 presents a summary of the literature which showed the non-Newtonian behavior of oil-based NFs.

## 4- Viscosity of oil-based nanofluids

The resistance of fluids against flowing is called viscosity, which affects the momentum transfer between the fluids' layers. One of the most important parameters, which has a certain effect on heat transfer of NFs, is, undoubtedly, the viscosity of NFs. It has a direct effect on the pressure loss and the pumping power. Various parameters affect the effective viscosity of NFs, such as the viscosity of the BF, solid concentration of NPs, particle diameter, shape, nature, and temperature. Although the thermal conductivity of the oil-based NFs has been widely investigated, the effective viscosity was not the focus of the researchers. Thus, to make a better understanding of the affecting

parameters on the viscosity, further research should be done. In the following sections, the effect of temperature and solid concentration of NPs on the effective viscosity of oil-based NF will be reviewed. Then the classical model to estimate the dynamic viscosity of NFs will be discussed. Finally, the proposed models by different researchers to predict the dynamic viscosity of different oil-based NFs, which are based on the experimental data, will be presented.

### 4-1- Effect of temperature and solid concentration

It is known that temperature and solid concentration of NPs are two important factors which have a certain effect on the viscosity behavior of NFs. The literature showed that adding NPs to the based fluids, even at a very low concentration, leads to increasing the dynamic viscosity of the NFs. However, there are some contradictory reports. The main cause of this increase would be that the possibility of growing the NPs' cluster is increased as the solid concentration increases. This nano-cluster would prevent the movement of the fluid layers easily, which leads to increasing the dynamic viscosity of the NFs. On the other hand, it has been proved that the dynamic viscosity decreases as the temperature increases. The main cause of this decrease would be attributed to the fact that the interactions among the fluid molecules weakening as the temperature increases.

Ettefaghi et al. [55] investigated the kinematic viscosity of MWCNT/engine oil (20W50) NF at two different temperatures of 40 ℃ and 100 ℃ and three concentrations of 0.1, 0.2, and 0.5 wt. %. They reported quiet interesting results; the kinematic viscosity decreased at the solid concentration of 0.1 wt. %, then it showed an increasing trend by increasing the solid concentration. They stated that at the low solid concentration (0.1 wt. %), the added nanotubes would place between the oil layers which leads to ease the movement of the oil layers and thus decreasing the viscosity of the NF. However, at higher concentrations (0.2 and 0.5 wt. %) the nanotubes start to agglomerate which leads to increasing the viscosity. They also reported that increasing the temperature leads to decreasing the kinematic viscosity. The maximum decrease was 0.25 % which occurred at the temperature of 100 ℃ and the solid concentration of 0.1 wt. % while the maximum increase was 1.7 % which took occurred at the temperature of 40 ℃ and the solid concentration of 0.5 wt. %.

The effects of temperature variations and solid concentration on the dynamic viscosity of MWCNT-MgO/engine oil (SAE50) has been studied by Asadi et al. [61]. They reported that increasing the solid concentration from 0 to 2 vol. % leads to a 65 % increase in the dynamic viscosity of the NF. It was the maximum increase in the dynamic viscosity which took place at the temperature of 40 ℃. They also reported that the minimum increase in the dynamic viscosity was 14.4 % which took

place at the solid concentration of 0.25 vol. % and temperature of 25 ℃. Fig. 8 displays the percentage of increase in dynamic viscosity of the NF in different temperatures and concentrations. They also reported that increasing the temperature from 25 to 50 ℃ caused approximately 77 % decrease in the dynamic viscosity of the NF in all the studied concentrations.

Hemmat Esfe et al. [63] studied the dynamic viscosity of MWCNT-$SiO_2$/engine oil (SAE40) hybrid NF in different temperatures and concentrations. They reported that increasing the NPs leads to increasing the dynamic viscosity of the NF which this increase in more noticeable in lower temperature compared to those higher. They reported the maximum increase of well over 30 % which accrued at the solid concentration of 1 vol. % and temperature of 40 ℃. Tab. 4 presents a summary of the recent literature of the dynamic viscosity of oil-based NFs.

### 4-2- Classical viscosity models

There are some classical models to predict the viscosity of suspensions. It is now well-established that most of them are not able to predict the viscosity enhancement of NFs with nanoparticle content except in rare cases or in the presence of aggregates. In this section, there are simply recalled in the following Tab. 5.

Undoubtedly, Einstein's model [66] is the most popular model which can be used to predict the viscosity of the suspensions containing spherical particles. The Einstein's model is as follows:

$$\mu_{eff} = \mu_{bf}(1+2.5\varphi) \quad (1)$$

The Einstein's model has been extended by Brinkman [67] to predict the viscosity of less diluted suspensions as follows:

$$\mu_{eff} = \mu_{bf}(1-\varphi)^{-2.5} \quad (1)$$

Considering the interactions among particles (Brownian motion) in the suspension, Batchelor [68] modified the Einstein's model as follows:

$$\mu_{eff} = \mu_{bf}(1+2.5\varphi+6.2\varphi^2) \quad (1)$$

Thus, a semi-experimental power-law model has been presented by Krieger and Dougherty [69] for the higher range in particle content as follows:

$$\mu_{nf} = \mu_{bf}\left(1-\frac{\varphi}{\varphi_m}\right)^{-[\mu]\varphi_m} \quad (1)$$

This model can predict the viscosity of the suspensions within any concentrations of spherical particles. Tab. 5 presents a summary of the classical model to predict the viscosity of suspensions containing different particles.

### 4-3- Proposed experimental models for oil-based nanofluids

Due to the fact that every nanoparticle has different properties such as density, specific heat capacity, and thermal conductivity, suspending these NPs in different BFs leads to different rheological and thermophysical properties of the resultant fluids (NF). Although many researchers tried to propose a model to predict the viscosity of different NFs, there are only a few models to predict the viscosity of NFs within the acceptable range of accuracy thus far. Thus researchers proposed different empirical-based correlations to predict the viscosity of a specific NF in the range of the studied temperatures, concentrations, shear rates, and so forth. In this section, a summary of the proposed correlation for estimating the viscosity of oil-based NF will be presented. It must be noted that almost all of these models have been proposed applying curve fitting method on the experimental data.

Pakdaman et al. [50] proposed a correlation to predict the kinematic viscosity of the MWCNT-heat transfer oil in terms of the studied range of temperatures (40 to 100 ℃) and concentrations (0.1, 0.2, and 0.4 wt. %). They employed the least square method to propose the correlation with the square correlation coefficient ($R^2$) of 0.91. The proposed correlation is as follows:

$$\frac{\nu_{nf}-\nu_{bf}}{\nu_{bf}} = (-11.23T + 5926.5)\varphi^{1.43} \quad (1)$$

In another experimental investigation, Dardan et al. [60] investigated the rheological properties of $Al_2O_3$-MWCNT/engine oil (SAE40) in different temperatures (25 to 50 ℃) and concentrations (0.0625 to 1 vol. %). Employing the curve fitting method (Marquardt-Levenberg algorithm [70]), they proposed a new correlation in terms of temperature and solid concentration to predict the dynamic viscosity of the NF within the range of the studied temperatures and concentrations. The proposed correlation is expressed as:

$$\frac{\mu_{nf}}{\mu_{bf}} = 1.123 + 0.3251\varphi - 0.08994T + 0.002552T^2 - 0.00002386T^3 + 0.9695\left(\frac{T}{\varphi}\right)^{0.01719} \quad (1)$$

It is interesting to note that the maximum error of the proposed correlation is reported as 2 %, which indicates the excellent accuracy of the correlation in predicting the dynamic viscosity of the NF.

Employing the curve fitting approach, Asadi et al. [61] proposed a new correlation regarding the temperature and solid concentration to predict the dynamic viscosity of MgO-MWCNT/engine oil (SAE50). The correlation can predict the dynamic viscosity of the studied NF in the temperatures of 25 to 50 ℃ and concentrations of 0.25 to 2 vol. % with the maximum error of 8 % (Fig. 9). The proposed correlation is as follows:

$$\mu_{nf} = 328201 \times T^{-2.053} \times \varphi^{0.09359} \quad (3)$$

A summary of the proposed models to estimate the viscosity of different oil-based NF is presented in Tab. 6.

## 5- Thermal conductivity

There is no disagreement that adding NPs, which possess different thermophysical properties, to conventional working fluids (i.e., water, ethylene glycol, oil, etc.) leads to changing the thermophysical properties of the conventional fluids. Thermal conductivity is one of the most important properties which has a direct effect on heat transfer performance of NFs. In this regard, various parameters affect the thermal conductivity of the resultant fluids (NFs); particle size & shape, temperature, thermal conductivity of the NPs, thermal conductivity of the BF, solid concentration of NPs, preparation techniques, additives (surfactants), acidity (pH) of the BF, and clustering. The effects of these parameters on thermophysical properties of different NFs was comprehensively reviewed by Gupta et al. [71]. Moreover, the responsible mechanisms for heat transport in NFs, which are Brownian motion, nanolayer, nanoclusters particle aggregation, liquid layering, and thermophoresis, was comprehensively discussed by Chandrasekar and Suresh [72], Fan and Wang [73], Pinto and Fiorelli [74], Tawfik [75], and Wong and Castillo [76]. Measuring the thermal conductivity of NFs, various methods have been employed by researchers such as transient hot-wire method, temperature oscillation method, 3-ω method, and the optical measurement method. However, the literature survey showed that the transient hot-wire method is

the dominant method used by researchers. In the following sections, the effect of adding different NPs on thermal conductivity of oil-based NFs will be reviewed and discussed. Then, the classical model to predict the thermal conductivity of NFs will be presented, and, finally, the proposed models by researchers to predict the thermal conductivity of different oil-based NFs will be presented.

### 4-1- Effect of adding nanoparticles

The literature showed that the thermal conductivity of NFs is higher compared to the BFs, and the oil-based NFs are not the exception. Researchers widely reported that increasing the solid concentration of NPs as well as the temperature leads to enhancing the thermal conductivity of NFs. Although the thermal conductivity of NFs plays a crucial role in heat transfer enhancement, there is a limited number of studies devoted to investigating the thermal conductivity of oil-based NFs. In this ground, the thermal conductivity of CuO/oil NF was investigated by Saeedinia et al. [49]. They measure the thermal conductivity in different temperatures (24 to 70 ℃) and two concentrations of 1 and 2 wt. %. They reported considerable enhancement in the thermal conductivity of the studied NF with temperature. With increasing the temperature in the suspension, the agglomeration of NPs diminishes, therefore, thermal conductivity enhances due to more uniformity of NPs in the mixture.

The effect of temperature and solid concentration on the thermal conductivity of oil-based NF containing graphite NPs was investigated by Wang et al. [54]. They reported that adding 1.36 vol. % graphite to the BF leads to 36 % enhancement in the thermal conductivity. It is reported that the thermal conductivity enhancement was nonlinear as the solid concentration increased. They also reported that the temperature has a weak effect on the thermal conductivity enhancement although increasing the temperature leads to increasing the thermal conductivity. They introduce the clustering effect as the dominant heat transfer mechanism.

Aberoumand et al. [40] studied the thermal conductivity of silver/heat transfer oil NF over different temperatures and concentrations. They reported that the thermal conductivity of the BF showed a decreasing trend as the temperature increased, but the thermal conductivity of the NF showed an inverse trend; it increases as the temperature increased. This increasing trend has been repeated for all the concentrations. They also indicated that the Brownian motion is the responsible mechanism to increase the thermal conductivity by increasing the temperature.

The effect of adding a different amount of Oleic Acid surfactant to $Al_2O_3$/diathermic oil NF on the thermal conductivity, in different temperatures (30 to 50 ℃) and three concentrations of 0.3, 0.7,

and 1 vol. %, has been investigated by Colangelo et al. [65]. Their results showed that adding surfactant does not affect the thermal conductivity of the NF. Moreover, increasing the solid concentration of the surfactant has also no effect on the thermal conductivity enhancement. They reported the maximum enhancement of 4 % at the solid concentration of 1 vol. %. A summary of the recent literature on the thermal conductivity of oil-based NF is presented in Tab. 7.

### 4-2- Classical thermal conductivity models

Many attempts have been made to present a model to predict and explain the thermal conductivity enhancement of suspensions and biphasic materials. In this ground, one of the pioneering studies was conducted by Maxwell [77]. He proposed the first theoretical model to predict the thermal conductivity of the suspensions containing large spherical particles as follows:

$$\frac{k_{nf}}{k_{bf}} = \frac{k_p + 2k_{bf} + 2(k_p - k_{bf})\varphi}{k_p + 2k_{bf} - (k_p - k_{bf})\varphi} \tag{1}$$

This is the base model to predict the thermal conductivity of homogeneous suspensions containing a low solid concentration of particles thus far. After this pioneering study, the Maxwell model was modified by Hamilton-Crosser who introduced and considered the shape factor of particles in the model:

$$k_{nf} = k_{bf}\left[\frac{\left(k_p + (n-1)k_{bf} + (n-1)\varphi(k_{bf} - k_p)\right)}{\left(k_p + (n-1)k_{bf} + \varphi(k_p - k_{bf})\right)}\right] \tag{2}$$

Where ***n*** represents the shape factor of the particles. It must be noted that for spherical particles $n$=3 while for other particle's shape, it differs from 0.5 to 6.

Another widely used model which is suitable for the suspensions containing a low solid concentration of spherical particles was introduced by Jeffrey [78]:

$$\frac{k_{nf}}{k_{bf}} = 1 + 3\beta\varphi + \left(3\beta^2 + \frac{3\beta^3}{4} + \frac{9\beta^3(\gamma+2)}{16(2\gamma+3)} + \frac{3\beta^4}{64} + \ldots\right)\varphi^2,$$

$$\beta = \frac{\gamma - 1}{\gamma + 2}, \tag{1}$$

$$\gamma = \frac{k_p}{k_{bf}}$$

Resulting in the better prediction compared to the models mentioned above for spherical particles, Bruggeman [79] proposed another model as follows:

$$\frac{k_{nf}}{k_{bf}} = \frac{1}{4}(3\varphi - 1)k_p + [(2-3\varphi)k_{bf}] + \frac{k_{bf}}{4}\sqrt{\Delta},$$
$$\Delta = \left[ (3\varphi-1)^2 \left(\frac{k_p}{k_{bf}}\right)^2 + [(2-3\varphi)^2 + 2(2+9\varphi-9\varphi^2)]\frac{k_p}{k_{bf}} \right] \quad (1)$$

More recently, considering both the static influence (Maxwell model [77]) and the effect of Brownian motion, Koo and Kleinstreuer [80] proposed the following model:

$$k_{nf} = k_{static} + k_{Brownian}$$
$$k_{static} = k_{bf}\left\{\frac{k_p + 2k_{bf} + 2(k_p - k_{bf})\varphi}{k_p + 2k_{bf} - (k_p - k_{bf})\varphi}\right\},$$
$$k_{Brownian} = 5\times10^4 \beta\varphi\rho_{bf} C_{P_{bf}} \sqrt{\frac{k_B T}{\rho_{nf} d_{np}} f}, \quad (1)$$
$$\beta = 0.0137(100\varphi)^{-0.8229} \quad \varphi < 1\%$$
$$\beta = 0.0017(100\varphi)^{-0.0841} \quad \varphi > 1\%$$
$$f = (-134.63 + 1722.3\varphi) + (0.4075 - 6.04\varphi)T$$

As for the hybrid NFs, the thermal conductivity can be predicted based on the principle of the mixture rule. The modified Maxwell model for the thermal conductivity of hybrid NF is:

$$k_{hnf} = k_{bf}\left[\frac{\frac{(k_{p1}\varphi_{p1} + k_{p2}\varphi_{p2})}{\varphi_{hnf}} + 2k_{bf} + 2(k_{p1}\varphi_{p1} + k_{p2}\varphi_{p2}) - 2\varphi k_{bf}}{\frac{(k_{p1}\varphi_{p1} + k_{p2}\varphi_{p2})}{\varphi_{hnf}} + 2k_{bf} - 2(k_{p1}\varphi_{p1} + k_{p2}\varphi_{p2}) - \varphi k_{bf}}\right] \quad (2)$$

It is proofed in the literature that none of the previous classical models (Eqs 12-14) can predict the thermal conductivity of different NFs within an acceptable range of accuracy and they generally underestimate thermal conductivity enhancement of NFs with nanoparticle loading. Thus researchers tried to proposed new empirical-based correlation to predict the thermal conductivity.

### 4-3- Proposed correlations

As it is discussed before (section 4-3), a different combination of NPs with working fluids results in having a NF which possesses different thermophysical properties compared to that of the based fluid. Various parameters, such as solid concentration of the particles, particle material, BF, particle size, particle shape, temperature, and acidity (pH), have a certain effect on the thermal conductivity of NFs. Thus researchers tried to proposed new correlations which can predict the thermal conductivity of specific NFs considering one or more of the mentioned affecting parameters. In this section, the empirical-based correlation, proposed so far, to predict the thermal conductivity of the oil-based NFs will be presented.

Pakdaman et al. [50] developed a correlation to predict the thermal conductivity of MWCNT/oil NF in terms of solid concentration of NPs, particle's size, and the bulk fluid temperature as follows:

$$\frac{k_{nf}}{k_{bf}} = 1 + 304.47(1+\varphi)^{136.35} \exp(-0.021T)\left(\frac{1}{d_p}\right)^{0.369}\left(\frac{T^{1.2321}}{10^{2.4642B/(T-C)}}\right) \quad (1)$$

Where the constant ***B*** and ***C*** are 247.8 and 140, respectively. It is interesting to note that the maximum deviation of this model is approximately 6 % which shows the accuracy of the correlation.

In another experimental study, Aberoumand et al. [40] proposed a new correlation to predict the thermal conductivity of Ag/oil NF over the temperatures ranging from 40 to 100 ℃ and concentrations of 0.12, 0.36, and 0.72 wt. %. They proposed the correlation in terms of solid concentration, temperature, and thermal conductivity of the nanoparticle with the maximum deviation of 3.5 % as follows:

$$k_{nf} = (3.6\times10^{-5}T - 0.0305)\varphi^2 + (0.086 - 1.6\times10^{-4}T)\varphi + 3.1\times10^{-4}T + 0.129 - 5.77\times10^{-6}k_p - 40\times10^{-4} \quad (1)$$

Ilyas et al. [81] proposed a new correlation to estimate the thermal conductivity of MWCNT-thermal oil NF in terms of solid concentration and temperature as follows:

$$k_{nf} = 0.595 - 0.4547(1-\varphi_p) + T\left[0.7422 - 0.606(1-\varphi_p) + \frac{0.2759}{(1-\varphi_p)} - \frac{0.3943}{(1-\varphi_p)^2}\right] \quad (1)$$

This correlation is valid within the temperatures ranging from 25 to 63.15 ℃ and concentrations ranging from 0.1 to 1 wt. %. Moreover, the mean absolute error and coefficient of determination ($R^2$) of the correlation have been reported as 3.5 % and 0.95, respectively.

Considering the solid concentration of NPs and temperature, Asadi et al. [82] proposed a new correlation to predict the thermal conductivity of $Al_2O_3$-MWCNT/oil hybrid NF in a different range of temperatures and concentrations with the maximum deviation of well under 2 % (Fig. 9) as follows:

$$k_{nf} = 0.1534 + 0.00026T + 1.1193\varphi \quad (20)$$

A summary of the proposed empirical-based correlation to predict the thermal conductivity of the oil-based NF has been presented in Tab. 8.

## 6- Density

Another important thermophysical property, which has a direct effect on Reynolds number, pressure loss, Nusselt number, and friction factor, is density. There are a limited number of studies on the density of NFs. Generally, the density of the NFs is predicted based on the mixture rule as follows [83]:

$$\rho_{nf} = \left(\frac{m}{V}\right)_{nf} = \frac{m_{bf} + m_{nf}}{V_{bf} + V_{nf}} = \frac{\rho_{bf} V_{bf} + \varphi_p V_p}{V_{bf} + V_p} \quad (21)$$

To predict the density of NFs, Pak and Cho [84], for the first time, used the following equation, which is for the micrometer-sized particles:

$$\rho_{nf} = \rho_p \varphi + (1-\varphi)\rho_{bf} \quad (21)$$

As for the density of hybrid NFs, extending the law of mixture, Takabi and Salehi [85] proposed the following equation, which showed good agreement with the experimental data:

$$\rho_{hnf} = \rho_{p1}\varphi_{p1} + \rho_{p2}\varphi_{p2} + (1-\varphi_h)\rho_{bf}; \quad \varphi_h = \varphi_{p1} + \varphi_{p2} \quad (21)$$

Saeedinia et al. [49] measured the density of CuO/oil NF in different concentrations ranging from 0.2 to 2 vol. %. They also compared the experimental data with those of Pak and Cho [84] correlation and declared that there is a good agreement between the experimental data and the correlation output.

In another experimental study, the density of MWCNT/oil NF has been measured by Pakdaman et al. [50]. They compared the experimental data with Pak and Cho [84] correlation and reported that there is only 1 % deviation between the experimental data and the correlation output.

Ilyas et al. [81] studied the density of MWCNT/oil NF is different concentrations (0.1 to 1 wt. %) and temperatures (20 to 60 ℃). They reported that the density of the NF showed a decreasing trend as the temperature increased. This trend was repeated in all the concentrations. Moreover, the density of the NF showed an increasing trend as the solid concentration increased. They also compared the experimental data with the Pak and Cho [84] correlation and found that there is a good agreement between the experimental data and the correlation output.

The density of $Al_2O_3$/oil NF was investigated by Ilyas et al. [86]. They conducted the experiment over different temperatures (20 to 60 ℃) and concentrations (0.5 to 3 wt. %). They compared the experimental results with those of Pak and Cho correlation and found that there is a good agreement between the experimental data and the correlation output in low concentrations while the difference was quite significant for the high concentrations. Based on the experimental data, they proposed a new correlation to predict the density of the NF in terms of temperature and solid concentration with the mean absolute error of ± 0.5 % and $R^2$=0.0997 as follows:

$$\rho_{nf} = -1012.83 - \frac{762.91}{T^{0.7125}} + 1578.311(1-\varphi_p)^{0.4211} + \frac{671.4463}{(1-\varphi_p)^{3.2992} T^{0.1938}} \quad (21)$$

From the available literature on the density of oil-based NFs, it can be concluded that the classical model presented by Pak and Cho [84] can predict the density of different NFs within the acceptable range of accuracy.

## 7- Specific heat capacity

Specific heat capacity, which is a parameter to shows the capability of a fluid to store and move the heat away from the hot source, is one of the most important properties that has a direct effect on the heat transfer performance of NFs. There are two models available in the literature to predict the specific heat capacity of NFs which are based on the law of mixture. The first model was presented by Pak and Cho [84] in terms of solid concentration of NPs, the specific heat capacity of NPs and BF:

$$c_{P_{nf}} = c_{P_P}\varphi + (1-\varphi)c_{P_{bf}} \quad (21)$$

The second model was presented by Xuan and Roetzel [87]. This model is based on the heat equilibrium as follows:

$$c_{P_{nf}} = (1-\varphi)\rho_{bf} c_{p_{bf}} + \varphi\rho_p c_{p_p} \quad (21)$$

As for the hybrid NFs, Takabi and Salehi [85] proposed a correlation to predict the specific heat capacity as follows:

$$c_{P_{hnf}} = \frac{(1-\varphi)\rho_{bf} c_{p_{bf}} + \varphi\rho_{p,1} c_{p_{p,1}} + \varphi\rho_{p,2} c_{p_{p,2}}}{\rho_{hnf}} \quad (21)$$

The specific heat capacity of CuO-oil NF over a different range of concentrations (0.2 to 2 wt. %) and temperatures (30 to 78 ℃) has been experimentally investigated by Saeedinia et al. [49]. They found that the specific heat of the studied NF is considerably less than that of the BF. They also reported that increasing the solid concentration of NPs leads to decreasing the specific heat capacity of the NF. They also compared the experimental results with Pak and Cho [84] and Xuan and Roetzel [87] correlations and reported that these models have no capability to predict the specific heat capacity of the studied NF; the models overestimate the specific heat of the NF.

Pakdaman et al. [50] experimentally investigated the specific heat capacity of MWCNT/heat transfer oil and compared the experimental findings with Pak and Cho [84] and Xuan and Roetzel correlations. They reported that these widely used correlations are not able to predict the specific heat capacity of the studied NF within the acceptable range of accuracy. Thus they proposed a new correlation to predict the specific heat capacity of the studied NF in terms of temperature and solid concentration as follows:

$$\frac{(c_{p_{bf}} - c_{p_{nf}})}{c_{p_{bf}}} = 0.0128T + 1.8382\varphi^{0.4779} \quad (21)$$

This correlation is valid over the studied range of temperatures (313 to 343 K) and concentrations (0.1, 0.2, and 0.4 wt. %). The maximum error of the proposed correlation is 9.4 % which shows the ability of the correlation to predict the specific heat capacity of the NF.

In another study, Ilyas et al. [81] developed a new correlation to predict the specific heat capacity of MWCNT/thermal oil NF in terms of temperature and solid concentration of NPs as follows:

$$c_{p_{nf}} = -20 + 21.573(1-\varphi_p) - 0.012T + 0.024T(1-\varphi_p) \quad (22)$$

The maximum deviation between the experimental data and the correlation output was reported as ± 3 %.

## 8- Discussion

An overview of different preparation methods of oil-based nanofluids have been presented in this review paper. It is seen that the two-step method is the dominant method used by researchers since it is the most economical approach for preparing the samples, especially in large quantity. Thermophysical properties of nanofluids play imperative role on heat transfer performance of the nanofluids. Dynamic viscosity directly affected the pumping power and pressure loss and thermal conductivity has direct effect on heat transfer performance. Various parameters have affect the dyna mic viscosity and thermal conductivity of nanofluid among which temperature and solid concentration of particles are the two imperative parameters. Adding nanoparticles to the oil (as a base fluid) results in increasing the dynamic viscosity of oil-based nanofluid; the main reason would be that adding nanoparticles leads to increasing the possibility of having large size clusters which prevents the easily movement of fluid layers. As for temperature, increasing the temperature leads to weakening the interactions among the fluid molecules which leads to decreasing the dynamic viscosity of the nanofluid. Adding nanoparticles, which possess higher thermal conductivity compared to the base fluid, results in improving the heat transfer performance of the base fluid. The dominant mechanisms of heat transfer performance are Brownian motion, nanoclusters particles aggregation, liquid layering, and thermophoresis, which are comprehensively discussed by Chandrasekar and Suresh [72], Fan and Wang [73], Pinto and Fiorelli [74], Tawfik [75], and Wong and Castillo [76]. It is also revealed that the transient hot-wire method is the dominant method for measuring the thermal conductivity of the oil-based nanofluids.

## 9- Concluding remarks and challenges

In the present paper, it is tried to review the different preparation techniques used in producing oil-based NFs as well the thermophysical properties of the oil-based NFs. It is found that the two-step method is the dominant method in the preparation of the oil-based NFs. However, the single/one-step method leads to preparing the more uniform and stable NFs. Moreover, it is revealed that oil-based NF possesses higher viscosity compared to that of the BF. This trend is similar as the solid concentration and temperature increases. However, in some limited cases such as [55], the viscosity of the NF showed a lower viscosity in the extremely low concentrations of particles (0.1 %wt)

compared to the BF. It would be a valuable path to conduct more in-depth investigations on the extremely low concentration of NPs. As for the thermal properties, it is found that adding NPs to the oil leads to enhancing the thermal conductivity of the BF. Increasing the solid concentration and temperature leads to increasing the thermal conductivity of the oil-based NF.

Reviewing the proposed classical models, it can be well understood that the classic models for predicting thermal conductivity and viscosity of nanofluids cannot be suitable for oil based nanofluids. According to Fig. 10, the proposed correlations are able to predict the viscosity while the predicted values by classic models are not matched with the measured data. These major deviations are because of the fact that several parameters such as volume concentration, bulk temperature of nanofluids, nanoparticle type, size and geometry, and even the base fluid certainly affect the viscosity while some of these parameters are not included in classic models. Because of the same reasons, classic models for predicting thermal conductivity are also unable to calculate thermal conductivity of oil based nanofluids. Moreover, thermal conductivity of oil based nanofluids increases with the temperature rising while all of the classic models predict thermal conductivity of all kinds of nanofluids (water, EG, oil, etc) in a decreasing way. This decreasing trend has come from the first experiments on nanofluids which was only water based. Thus, the models that have been derived from the water-based nanofluids cannot be used to predict thermal conductivity of other types of nanofluids such as oil based.

As for the density, it is revealed that adding NPs to BFs leads to increasing the density. However, increasing the temperature leads to decreasing the density of the NF. Furthermore, the literature showed that the proposed model by Pak and Cho [84] is able to predict the density of the oil-based NFs within the acceptable range of accuracy. Finally, it is found that adding NPs to conventional fluids leads to decreasing the specific heat of the fluid.

Further investigations could concentrate on studying the effects of different factors such as particle shape and size on thermophysical properties of oil-based NFs. Moreover, it would be of value to investigate the extremely low solid concentration of NPs and high temperatures (higher than 60 $^{o}$C) since such results are quite rare in the literature. Another future path would be focused on proposing models and correlations which consider more affecting key factors on thermophysical properties rather than just temperature and solid concentration of NPs.

## References


[1] O. Mahian, A. Kianifar, S. Z. Heris, D. Wen, A. Z. Sahin, and S. Wongwises, "Nanofluids effects on the evaporation rate in a solar still equipped with a heat exchanger," *Nano Energy*, vol. 36, pp. 134–155, Jun. 2017.

[2] A. Lenert and E. N. Wang, "Optimization of nanofluid volumetric receivers for solar thermal energy conversion," *Solar Energy*, vol. 86, no. 1, pp. 253–265, Jan. 2012.

[3] G. A. Oliveira, E. M. Cardenas Contreras, and E. P. Bandarra Filho, "Experimental study on the heat transfer of MWCNT/water nanofluid flowing in a car radiator," *Applied Thermal Engineering*, vol. 111, pp. 1450–1456, Jan. 2017.

[4] K. Goudarzi and H. Jamali, "Heat transfer enhancement of Al2O3-EG nanofluid in a car radiator with wire coil inserts," *Applied Thermal Engineering*, vol. 118, pp. 510–517, May 2017.

[5] S. R. Hosseini, M. Sheikholeslami, M. Ghasemian, and D. D. Ganji, "Nanofluid heat transfer analysis in a microchannel heat sink (MCHS) under the effect of magnetic field by means of KKL model," *Powder Technology*, vol. 324, pp. 36–47, Jan. 2018.

[6] A. Arabpour, A. Karimipour, and D. Toghraie, "The study of heat transfer and laminar flow of kerosene/multi-walled carbon nanotubes (MWCNTs) nanofluid in the microchannel heat sink with slip boundary condition," *Journal of Thermal Analysis and Calorimetry*, vol. 131, no. 2, pp. 1553–1566, Feb. 2018.

[7] H. Saleh, E. Alali, and A. Ebaid, "Medical applications for the flow of carbon-nanotubes suspended nanofluids in the presence of convective condition using Laplace transform," *Journal of the Association of Arab Universities for Basic and Applied Sciences*, vol. 24, no. 1, pp. 206–212, Oct. 2017.

[8] A. A. Alnaqi, S. Aghakhani, A. H. Pordanjani, R. Bakhtiari, A. Asadi, and M. Tran, "Effects of magnetic field on the convective heat transfer rate and entropy generation of a nanofluid in an inclined square cavity equipped with a conductor fin: Considering the radiation effect," *International Journal of Heat and Mass Transfer*, 2019.

[9] A. Moradikazerouni, M. Afrand, J. Alsarraf, S. Wongwises, A. Asadi, and T. K. Nguyen, "Investigation of a computer CPU heat sink under laminar forced convection using a structural stability method," *International Journal of Heat and Mass Transfer*, vol. 134, pp. 1218–1226, May 2019.

[10] A. Ahmadi Nadooshan, H. Eshgarf, and M. Afrand, "Evaluating the effects of different parameters on rheological behavior of nanofluids: A comprehensive review," *Powder Technology*, vol. 338, pp. 342–353, Oct. 2018.

[11] H. M. Ali *et al.*, "Preparation Techniques of TiO2 Nanofluids and Challenges: A Review," *Applied Sciences*, vol. 8, no. 4, p. 587, Apr. 2018.

[12] M. U. Sajid and H. M. Ali, "Recent advances in application of nanofluids in heat transfer devices: A critical review," *Renewable and Sustainable Energy Reviews*, vol. 103, pp. 556–592, Apr. 2019.

[13] O. Mahian, A. Kianifar, S. A. Kalogirou, I. Pop, and S. Wongwises, "A review of the applications of nanofluids in solar energy," *International Journal of Heat and Mass Transfer*,

vol. 57, no. 2, pp. 582–594, Feb. 2013.

[14] H. Babar, M. Sajid, and H. Ali, "Viscosity of hybrid nanofluids: A critical review," *Thermal Science*, no. 00, pp. 15–15, 2019.

[15] A. J. Chamkha, M. Molana, A. Rahnama, and F. Ghadami, "On the nanofluids applications in microchannels: A comprehensive review," *Powder Technology*, vol. 332, pp. 287–322, Jun. 2018.

[16] S. Izadi, T. Armaghani, R. Ghasemiasl, A. J. Chamkha, and M. Molana, "A comprehensive review on mixed convection of nanofluids in various shapes of enclosures," *Powder Technology*, vol. 343, pp. 880–907, Feb. 2019.

[17] O. Mahian *et al.*, "Recent Advances in Modeling and Simulation of Nanofluid Flows-Part I: Fundamental and Theory," *Phys*, 2018.

[18] O. Mahian *et al.*, "Recent advances in modeling and simulation of nanofluid flows—Part II: Applications," *Physics Reports*, Dec. 2018.

[19] H. Babar and H. M. Ali, "Towards hybrid nanofluids: Preparation, thermophysical properties, applications, and challenges," *Journal of Molecular Liquids*, Feb. 2019.

[20] E. Bellos and C. Tzivanidis, "Investigation of a nanofluid-based concentrating thermal photovoltaic with a parabolic reflector," *Energy Conversion and Management*, vol. 180, pp. 171–182, Jan. 2019.

[21] E. Bellos, C. Tzivanidis, and D. Tsimpoukis, "Thermal, hydraulic and exergetic evaluation of a parabolic trough collector operating with thermal oil and molten salt based nanofluids," *Energy Conversion and Management*, vol. 156, pp. 388–402, Jan. 2018.

[22] R. Loni, E. A. Asli-Ardeh, B. Ghobadian, A. B. Kasaeian, and E. Bellos, "Energy and exergy investigation of alumina/oil and silica/oil nanofluids in hemispherical cavity receiver: Experimental Study," *Energy*, vol. 164, pp. 275–287, Dec. 2018.

[23] R. Loni, E. Askari Asli-Ardeh, B. Ghobadian, A. B. Kasaeian, and E. Bellos, "Thermal performance comparison between Al2O3/oil and SiO2/oil nanofluids in cylindrical cavity receiver based on experimental study," *Renewable Energy*, vol. 129, pp. 652–665, Dec. 2018.

[24] N. A. Che Sidik, M. Mahmud Jamil, W. M. A. Aziz Japar, and I. Muhammad Adamu, "A review on preparation methods, stability and applications of hybrid nanofluids," *Renewable and Sustainable Energy Reviews*, vol. 80, pp. 1112–1122, Dec. 2017.

[25] C.-H. Lo, T.-T. Tsung, L.-C. Chen, C.-H. Su, and H.-M. Lin, "Fabrication of copper oxide nanofluid using submerged arc nanoparticle synthesis system (SANSS)," *Journal of Nanoparticle Research*, vol. 7, no. 2–3, pp. 313–320, Jun. 2005.

[26] J. A. Choi, S.U.S.; Eastman, "Enhancing thermal conductivity of fluids with nanoparticles, ASME FED, 231: 99–103," *International mechanical engineering congress and exhibition, San Francisco, CA (United States)*, 1995.

[27] M. T. Jamal-Abad, A. Zamzamian, and M. Dehghan, "Experimental studies on the heat transfer and pressure drop characteristics of Cu–water and Al–water nanofluids in a spiral coil," *Experimental Thermal and Fluid Science*, vol. 47, pp. 206–212, May 2013.

[28] L. Godson, K. Deepak, C. Enoch, B. Jefferson, and B. Raja, "Heat transfer characteristics of silver/water nanofluids in a shell and tube heat exchanger," *Archives of Civil and Mechanical Engineering*, vol. 14, no. 3, pp. 489–496, May 2014.

[29] M. Sahooli and S. Sabbaghi, "Investigation of thermal properties of CuO nanoparticles on the ethylene glycol–water mixture," *Materials Letters*, vol. 93, pp. 254–257, Feb. 2013.

[30] C.-Y. Lin, J.-C. Wang, and T.-C. Chen, "Analysis of suspension and heat transfer characteristics of Al2O3 nanofluids prepared through ultrasonic vibration," *Applied Energy*, vol. 88, no. 12, pp. 4527–4533, Dec. 2011.

[31] Y.-H. Hung, T.-P. Teng, T.-C. Teng, and J.-H. Chen, "Assessment of heat dissipation performance for nanofluid," *Applied Thermal Engineering*, vol. 32, pp. 132–140, Jan. 2012.

[32] S. Suresh, M. Chandrasekar, and P. Selvakumar, "Experimental studies on heat transfer and friction factor characteristics of CuO/water nanofluid under laminar flow in a helically dimpled tube," *Heat and Mass Transfer*, vol. 48, no. 4, pp. 683–694, Apr. 2012.

[33] S. Suresh, P. Selvakumar, M. Chandrasekar, and V. S. Raman, "Experimental studies on heat transfer and friction factor characteristics of Al2O3/water nanofluid under turbulent flow with spiraled rod inserts," *Chemical Engineering and Processing: Process Intensification*, vol. 53, pp. 24–30, Mar. 2012.

[34] J. A. Eastman, S. U. S. Choi, S. Li, W. Yu, and L. J. Thompson, "Anomalously increased effective thermal conductivities of ethylene glycol-based nanofluids containing copper nanoparticles," *Applied Physics Letters*, vol. 78, no. 6, pp. 718–720, Feb. 2001.

[35] Y.-J. Chen, P.-Y. Wang, Z.-H. Liu, and Y.-Y. Li, "Heat transfer characteristics of a new type of copper wire-bonded flat heat pipe using nanofluids," *International Journal of Heat and Mass Transfer*, vol. 67, pp. 548–559, Dec. 2013.

[36] M. N. Pantzali, A. A. Mouza, and S. V. Paras, "Investigating the efficacy of nanofluids as coolants in plate heat exchangers (PHE)," *Chemical Engineering Science*, vol. 64, no. 14, pp. 3290–3300, Jul. 2009.

[37] S. S. Chougule and S. K. Sahu, "Comparative Study of Cooling Performance of Automobile Radiator Using $Al_2O_3$ -Water and Carbon Nanotube-Water Nanofluid," *Journal of Nanotechnology in Engineering and Medicine*, vol. 5, no. 1, p. 010901, Mar. 2014.

[38] S. S. Chougule and S. K. Sahu, "Thermal Performance of Automobile Radiator Using Carbon Nanotube-Water Nanofluid—Experimental Study," *Journal of Thermal Science and Engineering Applications*, vol. 6, no. 4, p. 041009, Jun. 2014.

[39] L. S. Sundar, M. K. Singh, I. Bidkin, and A. C. M. Sousa, "Experimental investigations in heat transfer and friction factor of magnetic Ni nanofluid flowing in a tube," *International Journal of Heat and Mass Transfer*, vol. 70, pp. 224–234, Mar. 2014.

[40] S. Aberoumand, A. Jafarimoghaddam, M. Moravej, H. Aberoumand, and K. Javaherdeh, "Experimental study on the rheological behavior of silver-heat transfer oil nanofluid and suggesting two empirical based correlations for thermal conductivity and viscosity of oil based nanofluids," *Applied Thermal Engineering*, vol. 101, pp. 362–372, May 2016.

[41] S. Aberoumand and A. Jafarimoghaddam, "Experimental study on synthesis, stability, thermal conductivity and viscosity of Cu–engine oil nanofluid," *Journal of the Taiwan*

*Institute of Chemical Engineers*, vol. 71, pp. 315–322, Feb. 2017.

[42] M. R. Raveshi, A. Keshavarz, M. S. Mojarrad, and S. Amiri, "Experimental investigation of pool boiling heat transfer enhancement of alumina–water–ethylene glycol nanofluids," *Experimental Thermal and Fluid Science*, vol. 44, pp. 805–814, Jan. 2013.

[43] M. Naraki, S. M. Peyghambarzadeh, S. H. Hashemabadi, and Y. Vermahmoudi, "Parametric study of overall heat transfer coefficient of CuO/water nanofluids in a car radiator," *International Journal of Thermal Sciences*, vol. 66, pp. 82–90, Apr. 2013.

[44] S. Halelfadl, T. Maré, and P. Estellé, "Efficiency of carbon nanotubes water based nanofluids as coolants," *Experimental Thermal and Fluid Science*, vol. 53, pp. 104–110, Feb. 2014.

[45] A. Zamzamian, S. N. Oskouie, A. Doosthoseini, A. Joneidi, and M. Pazouki, "Experimental investigation of forced convective heat transfer coefficient in nanofluids of Al2O3/EG and CuO/EG in a double pipe and plate heat exchangers under turbulent flow," *Experimental Thermal and Fluid Science*, vol. 35, no. 3, pp. 495–502, Apr. 2011.

[46] T.-P. Teng and C.-C. Yu, "Heat dissipation performance of MWCNTs nano-coolant for vehicle," *Experimental Thermal and Fluid Science*, vol. 49, pp. 22–30, Sep. 2013.

[47] S. Zeinali Heris, T. H. Nassan, S. H. Noie, H. Sardarabadi, and M. Sardarabadi, "Laminar convective heat transfer of Al2O3/water nanofluid through square cross-sectional duct," *International Journal of Heat and Fluid Flow*, vol. 44, pp. 375–382, Dec. 2013.

[48] M. Ghanbarpour, E. Bitaraf Haghigi, and R. Khodabandeh, "Thermal properties and rheological behavior of water based Al2O3 nanofluid as a heat transfer fluid," *Experimental Thermal and Fluid Science*, vol. 53, pp. 227–235, Feb. 2014.

[49] M. Saeedinia, M. A. Akhavan-Behabadi, and P. Razi, "Thermal and rheological characteristics of CuO–Base oil nanofluid flow inside a circular tube," *International Communications in Heat and Mass Transfer*, vol. 39, no. 1, pp. 152–159, Jan. 2012.

[50] M. Fakoor Pakdaman, M. A. Akhavan-Behabadi, and P. Razi, "An experimental investigation on thermo-physical properties and overall performance of MWCNT/heat transfer oil nanofluid flow inside vertical helically coiled tubes," *Experimental Thermal and Fluid Science*, vol. 40, pp. 103–111, Jul. 2012.

[51] M. Afrand, D. Toghraie, and B. Ruhani, "Effects of temperature and nanoparticles concentration on rheological behavior of Fe3O4–Ag/EG hybrid nanofluid: An experimental study," *Experimental Thermal and Fluid Science*, vol. 77, pp. 38–44, Oct. 2016.

[52] D. Toghraie, S. M. Alempour, and M. Afrand, "Experimental determination of viscosity of water based magnetite nanofluid for application in heating and cooling systems," *Journal of Magnetism and Magnetic Materials*, vol. 417, pp. 243–248, Nov. 2016.

[53] M. Hemmat Esfe, S. Saedodin, A. Asadi, and A. Karimipour, "Thermal conductivity and viscosity of Mg(OH)2-ethylene glycol nanofluids," *Journal of Thermal Analysis and Calorimetry*, vol. 120, no. 2, pp. 1145–1149, May 2015.

[54] B. Wang, X. Wang, W. Lou, and J. Hao, "Thermal conductivity and rheological properties of graphite/oil nanofluids," *Colloids and Surfaces A: Physicochemical and Engineering Aspects*, vol. 414, pp. 125–131, Nov. 2012.

[55] E. Ettefaghi, H. Ahmadi, A. Rashidi, A. Nouralishahi, and S. S. Mohtasebi, "Preparation and thermal properties of oil-based nanofluid from multi-walled carbon nanotubes and engine oil as nano-lubricant," *International Communications in Heat and Mass Transfer*, vol. 46, pp. 142–147, Aug. 2013.

[56] B. Wei, C. Zou, X. Yuan, and X. Li, "Thermo-physical property evaluation of diathermic oil based hybrid nanofluids for heat transfer applications," *International Journal of Heat and Mass Transfer*, vol. 107, pp. 281–287, Apr. 2017.

[57] M. Asadi and A. Asadi, "Dynamic viscosity of MWCNT/ZnO-engine oil hybrid nanofluid: An experimental investigation and new correlation in different temperatures and solid concentrations," *International Communications in Heat and Mass Transfer*, 2016.

[58] A. Alirezaie, S. Saedodin, M. H. Esfe, and S. H. Rostamian, "Investigation of rheological behavior of MWCNT (COOH-functionalized)/MgO - Engine oil hybrid nanofluids and modelling the results with artificial neural networks," *Journal of Molecular Liquids*, vol. 241, pp. 173–181, Sep. 2017.

[59] M. Farbod, R. Kouhpeymani asl, and A. R. Noghreh abadi, "Morphology dependence of thermal and rheological properties of oil-based nanofluids of CuO nanostructures," *Colloids and Surfaces A: Physicochemical and Engineering Aspects*, vol. 474, pp. 71–75, Jun. 2015.

[60] E. Dardan, M. Afrand, and A. H. Meghdadi Isfahani, "Effect of suspending hybrid nano-additives on rheological behavior of engine oil and pumping power," *Applied Thermal Engineering*, vol. 109, pp. 524–534, Oct. 2016.

[61] A. Asadi, M. Asadi, M. Rezaei, M. Siahmargoi, and F. Asadi, "The effect of temperature and solid concentration on dynamic viscosity of MWCNT/MgO (20–80)–SAE50 hybrid nano-lubricant and proposing a new correlation: An experimental study," *International Communications in Heat and Mass Transfer*, vol. 78, 2016.

[62] R. P. Chhabra, "Non-Newtonian Fluids: An Introduction," in *Rheology of Complex Fluids*, New York, NY: Springer New York, 2010, pp. 3–34.

[63] M. Hemmat Esfe, M. Afrand, W.-M. Yan, H. Yarmand, D. Toghraie, and M. Dahari, "Effects of temperature and concentration on rheological behavior of MWCNTs/SiO2(20–80)-SAE40 hybrid nano-lubricant," *International Communications in Heat and Mass Transfer*, vol. 76, pp. 133–138, Aug. 2016.

[64] K. Anoop, R. Sadr, R. Yrac, and M. Amani, "High-pressure rheology of alumina-silicone oil nanofluids," *Powder Technology*, vol. 301, pp. 1025–1031, Nov. 2016.

[65] G. Colangelo, E. Favale, P. Miglietta, M. Milanese, and A. de Risi, "Thermal conductivity, viscosity and stability of Al2O3-diathermic oil nanofluids for solar energy systems," *Energy*, vol. 95, pp. 124–136, Jan. 2016.

[66] A. E.-A. Phys. and undefined 1906, "A new determination of molecular dimensions," *ci.nii.ac.jp*.

[67] H. C. Brinkman, "The Viscosity of Concentrated Suspensions and Solutions," *The Journal of Chemical Physics*, vol. 20, no. 4, pp. 571–571, Apr. 1952.

[68] G. K. Batchelor, "The effect of Brownian motion on the bulk stress in a suspension of spherical particles," *Journal of Fluid Mechanics*, vol. 83, no. 01, p. 97, Nov. 1977.

[69] I. M. Krieger and T. J. Dougherty, “A Mechanism for Non- Newtonian Flow in Suspensions of Rigid Spheres,” *Transactions of the Society of Rheology*, vol. 3, no. 1, pp. 137–152, Mar. 1959.

[70] D. W. Marquardt, “AN ALGORITHM FOR LEAST-SQUARES ESTIMATION OF NONLINEAR PARAMETERS*,” 1963.

[71] M. Gupta, V. Singh, R. Kumar, and Z. Said, “A review on thermophysical properties of nanofluids and heat transfer applications,” *Renewable and Sustainable Energy Reviews*, vol. 74, pp. 638–670, Jul. 2017.

[72] M. Chandrasekar and S. Suresh, “A Review on the Mechanisms of Heat Transport in Nanofluids,” *Heat Transfer Engineering*, vol. 30, no. 14, pp. 1136–1150, Dec. 2009.

[73] J. Fan and L. Wang, “Review of Heat Conduction in Nanofluids,” *Journal of Heat Transfer*, vol. 133, no. 4, p. 040801, Apr. 2011.

[74] R. V. Pinto and F. A. S. Fiorelli, “Review of the mechanisms responsible for heat transfer enhancement using nanofluids,” *Applied Thermal Engineering*, vol. 108, pp. 720–739, Sep. 2016.

[75] M. M. Tawfik, “Experimental studies of nanofluid thermal conductivity enhancement and applications: A review,” *Renewable and Sustainable Energy Reviews*, vol. 75, pp. 1239–1253, Aug. 2017.

[76] K. V. Wong and M. J. Castillo, “Heat Transfer Mechanisms and Clustering in Nanofluids,” *Advances in Mechanical Engineering*, vol. 2, p. 795478, Jan. 2010.

[77] J. Maxwell, “A treatise on electricity and magnetism,” 1881.

[78] ( ’ Communicated and G. K. Batchelor, “Conduction through a random suspension of spheres,” 1973.

[79] BRUGGEMAN and DAG., “The calculation of various physical constants of heterogeneous substances. I. The dielectric constants and conductivities of mixtures composed of isotropic substances,” *Annals of Physics*, vol. 416, pp. 636–791, 1935.

[80] J. Koo and C. Kleinstreuer, “A new thermal conductivity model for nanofluids,” *Journal of Nanoparticle Research*, vol. 6, no. 6, pp. 577–588, Dec. 2004.

[81] S. U. Ilyas, R. Pendyala, and M. Narahari, “Stability and thermal analysis of MWCNT-thermal oil-based nanofluids,” *Colloids and Surfaces A: Physicochemical and Engineering Aspects*, vol. 527, pp. 11–22, Aug. 2017.

[82] A. Asadi, M. Asadi, A. Rezaniakolaei, L. A. Rosendahl, M. Afrand, and S. Wongwises, “Heat transfer efficiency of Al2O3-MWCNT/thermal oil hybrid nanofluid as a cooling fluid in thermal and energy management applications: An experimental and theoretical investigation,” *International Journal of Heat and Mass Transfer*, vol. 117, pp. 474–486, Feb. 2018.

[83] J. A. Ranga Babu, K. K. Kumar, and S. Srinivasa Rao, “State-of-art review on hybrid nanofluids,” *Renewable and Sustainable Energy Reviews*, vol. 77, pp. 551–565, Sep. 2017.

[84] B. C. Pak and Y. I. Cho, “HYDRODYNAMIC AND HEAT TRANSFER STUDY OF

DISPERSED FLUIDS WITH SUBMICRON METALLIC OXIDE PARTICLES," *Experimental Heat Transfer*, vol. 11, no. 2, pp. 151–170, Apr. 1998.

[85] B. Takabi and S. Salehi, "Augmentation of the Heat Transfer Performance of a Sinusoidal Corrugated Enclosure by Employing Hybrid Nanofluid," *Advances in Mechanical Engineering*, vol. 6, p. 147059, Jan. 2014.

[86] S. U. Ilyas, R. Pendyala, M. Narahari, and L. Susin, "Stability, rheology and thermal analysis of functionalized alumina- thermal oil-based nanofluids for advanced cooling systems," *Energy Conversion and Management*, vol. 142, pp. 215–229, Jun. 2017.

[87] Y. Xuan and W. Roetzel, "Conceptions for heat transfer correlation of nanofluids," *International Journal of Heat and Mass Transfer*, vol. 43, no. 19, pp. 3701–3707, Oct. 2000.

[88] S. S. Botha, P. Ndungu, and B. J. Bladergroen, "Physicochemical Properties of Oil-Based Nanofluids Containing Hybrid Structures of Silver Nanoparticles Supported on Silica," *Industrial & Engineering Chemistry Research*, vol. 50, no. 6, pp. 3071–3077, Mar. 2011.

[89] M. Hemmat Esfe, R. Karimpour, A. A. Abbasian Arani, and J. Shahram, "Experimental investigation on non-Newtonian behavior of Al2O3-MWCNT/5W50 hybrid nano-lubricant affected by alterations of temperature, concentration and shear rate for engine applications," *International Communications in Heat and Mass Transfer*, vol. 82, pp. 97–102, Mar. 2017.

[90] M. Afrand, K. Nazari Najafabadi, and M. Akbari, "Effects of temperature and solid volume fraction on viscosity of SiO2-MWCNTs/SAE40 hybrid nanofluid as a coolant and lubricant in heat engines," *Applied Thermal Engineering*, vol. 102, pp. 45–54, Jun. 2016.

[91] X. Li, C. Zou, L. Zhou, and A. Qi, "Experimental study on the thermo-physical properties of diathermic oil based SiC nanofluids for high temperature applications," *International Journal of Heat and Mass Transfer*, vol. 97, pp. 631–637, Jun. 2016.

[92] M. Hemmat Esfe, M. Afrand, S. H. Rostamian, and D. Toghraie, "Examination of rheological behavior of MWCNTs/ZnO-SAE40 hybrid nano-lubricants under various temperatures and solid volume fractions," *Experimental Thermal and Fluid Science*, vol. 80, pp. 384–390, Jan. 2017.

[93] W. Li, C. Zou, and X. Li, "Thermo-physical properties of waste cooking oil-based nanofluids," *Applied Thermal Engineering*, vol. 112, pp. 784–792, Feb. 2017.

[94] A. Asadi and F. Pourfattah, "Heat transfer performance of two oil-based nanofluids containing ZnO and MgO nanoparticles; a comparative experimental investigation," *Powder Technology*, vol. 343, pp. 296–308, 2019.

[95] A. Ahmadi Nadooshan, M. Hemmat Esfe, and M. Afrand, "Evaluation of rheological behavior of 10W40 lubricant containing hybrid nano-material by measuring dynamic viscosity," *Physica E: Low-dimensional Systems and Nanostructures*, vol. 92, pp. 47–54, Aug. 2017.

[96] A. Asadi, "A guideline towards easing the decision-making process in selecting an effective nanofluid as a heat transfer fluid," *Energy Conversion and Management*, vol. 175, 2018.

[97] M. Hemmat Esfe, S. Saedodin, M. Rejvani, and J. Shahram, "Experimental investigation, model development and sensitivity analysis of rheological behavior of ZnO/10W40 nano-lubricants for automotive applications," *Physica E: Low-dimensional Systems and*

*Nanostructures*, vol. 90, pp. 194–203, Jun. 2017.

[98] M. A. Moghaddam and K. Motahari, "Experimental investigation, sensitivity analysis and modeling of rheological behavior of MWCNT-CuO (30–70)/SAE40 hybrid nano-lubricant," *Applied Thermal Engineering*, vol. 123, pp. 1419–1433, Aug. 2017.

[99] A. Asadi, M. Asadi, A. Rezaniakolaei, L. A. Rosendahl, and S. Wongwises, "An experimental and theoretical investigation on heat transfer capability of Mg (OH)<inf>2</inf>/MWCNT-engine oil hybrid nano-lubricant adopted as a coolant and lubricant fluid," *Applied Thermal Engineering*, vol. 129, 2018.

[100] K. Motahari, M. Abdollahi Moghaddam, and M. Moradian, "Experimental investigation and development of new correlation for influences of temperature and concentration on dynamic viscosity of MWCNT-SiO2 (20-80)/20W50 hybrid nano-lubricant," *Chinese Journal of Chemical Engineering*, vol. 26, no. 1, pp. 152–158, Jan. 2018.

[101] M. Hemmat Esfe and H. Rostamian, "Non-Newtonian power-law behavior of TiO2/SAE 50 nano-lubricant: An experimental report and new correlation," *Journal of Molecular Liquids*, vol. 232, pp. 219–225, Apr. 2017.

[102] M. Hemmat Esfe, H. Rostamian, M. Rejvani, and M. R. S. Emami, "Rheological behavior characteristics of ZrO2-MWCNT/10w40 hybrid nano-lubricant affected by temperature, concentration, and shear rate: An experimental study and a neural network simulating," *Physica E: Low-dimensional Systems and Nanostructures*, vol. 102, pp. 160–170, Aug. 2018.

[103] Y. H. Chai, S. Yusup, V. S. Chok, S. Irawan, and J. S. D. B. Singh, "Thermophysical properties of graphene nanosheets – Hydrogenated oil based nanofluid for drilling fluid improvements," *Applied Thermal Engineering*, vol. 122, pp. 794–805, Jul. 2017.

[104] M. Hemmat Esfe and S. Esfandeh, "Investigation of rheological behavior of hybrid oil based nanolubricant-coolant applied in car engines and cooling equipments," *Applied Thermal Engineering*, vol. 131, pp. 1026–1033, Feb. 2018.

[105] H. Attari, F. Derakhshanfard, and M. H. K. Darvanjooghi, "Effect of temperature and mass fraction on viscosity of crude oil-based nanofluids containing oxide nanoparticles," *International Communications in Heat and Mass Transfer*, vol. 82, pp. 103–113, Mar. 2017.

[106] "THE GENERAL THEORY OF VISCOSITY."

[107] H. Brenner and D. W. Condiff, "Transport mechanics in systems of orientable particles. IV. convective transport," *Journal of Colloid and Interface Science*, vol. 47, no. 1, pp. 199–264, Apr. 1974.

[108] D. J. Jeffrey and A. Acrivos, "The rheological properties of suspensions of rigid particles," *AIChE Journal*, vol. 22, no. 3, pp. 417–432, May 1976.

[109] X. Wang, X. Xu, and S. U. S. Choi, "Thermal Conductivity of Nanoparticle - Fluid Mixture," *Journal of Thermophysics and Heat Transfer*, vol. 13, no. 4, pp. 474–480, Oct. 1999.

[110] A. L. Graham, "On the viscosity of suspensions of solid spheres," *Applied Scientific Research*, vol. 37, no. 3–4, pp. 275–286, 1981.

[111] L. E. Nielsen, "Generalized Equation for the Elastic Moduli of Composite Materials," *Journal of Applied Physics*, vol. 41, no. 11, pp. 4626–4627, Oct. 1970.

**Figures:**

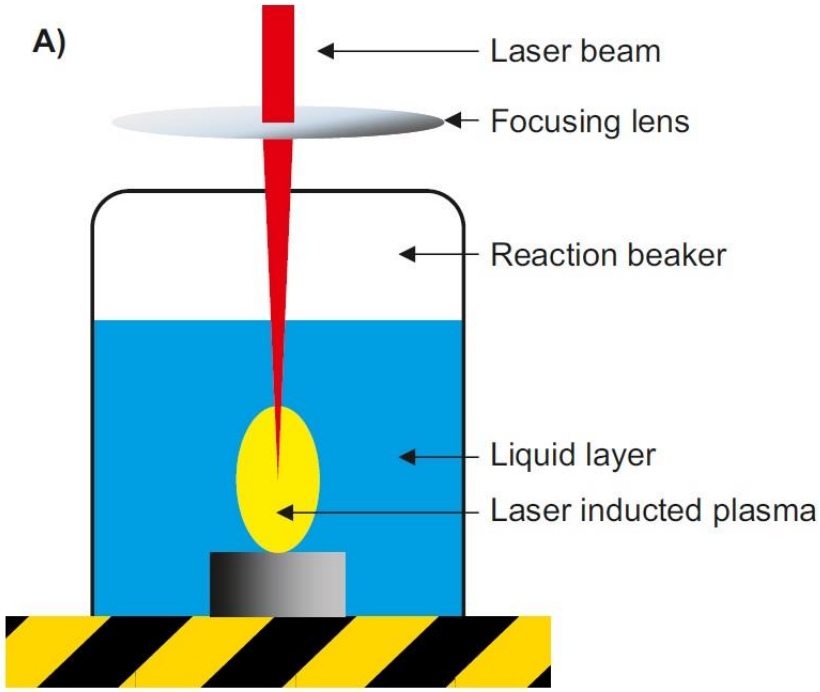

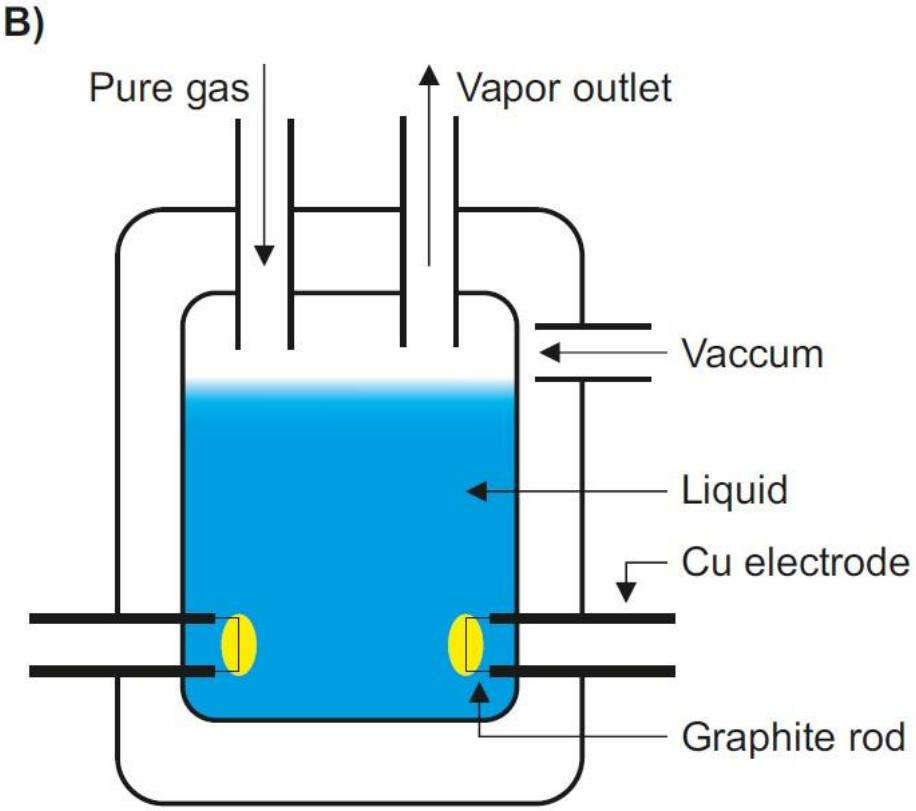


**Fig. 1 A) A schematic view of the laser ablation apparatus, B) A schematic view of the submerged arc method to synthesis the NPs**

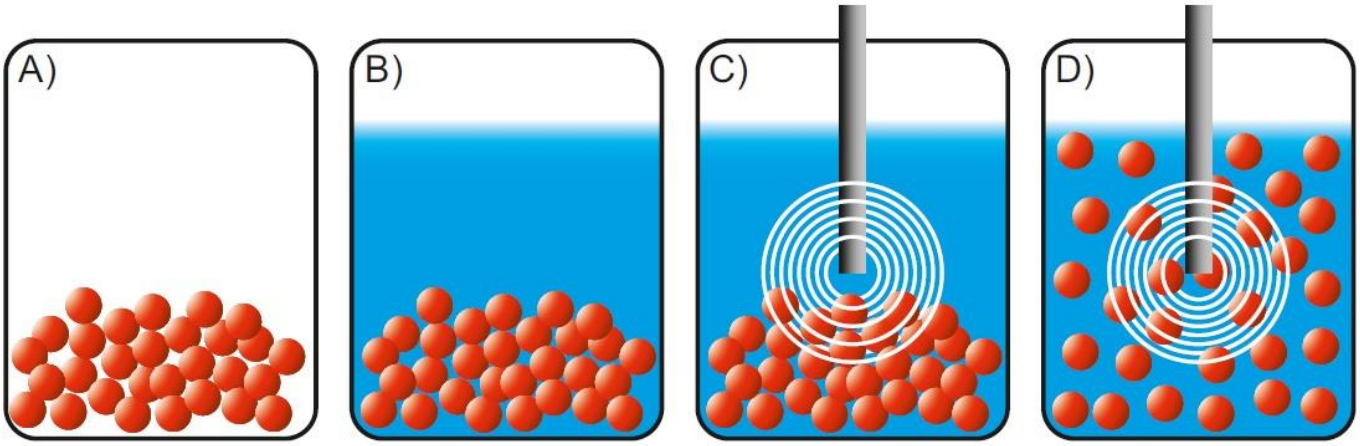


**Fig. 2 Schematic view of the two-step NF preparation process; A) Nanoparticle synthesis/preparation, B) base fluid adding, C) surfactant adding and ultrasonication of agglomerated particles, D) stable NF**

A

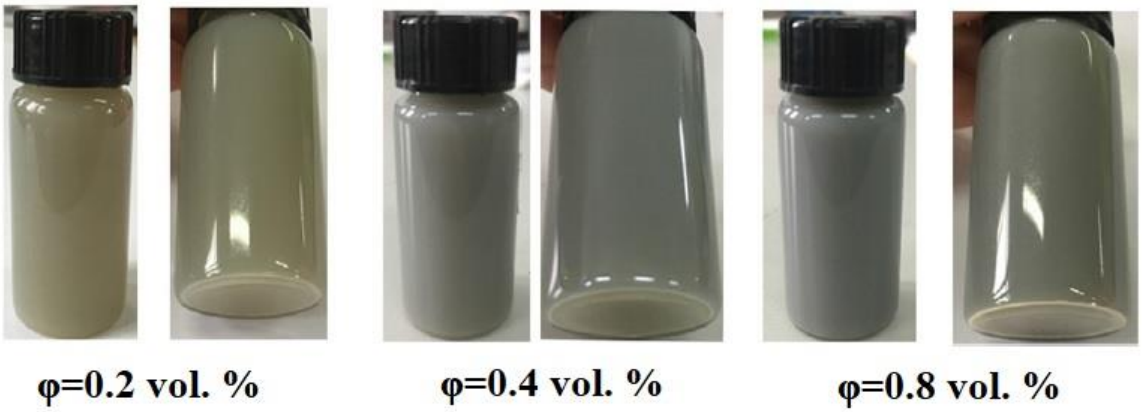


B

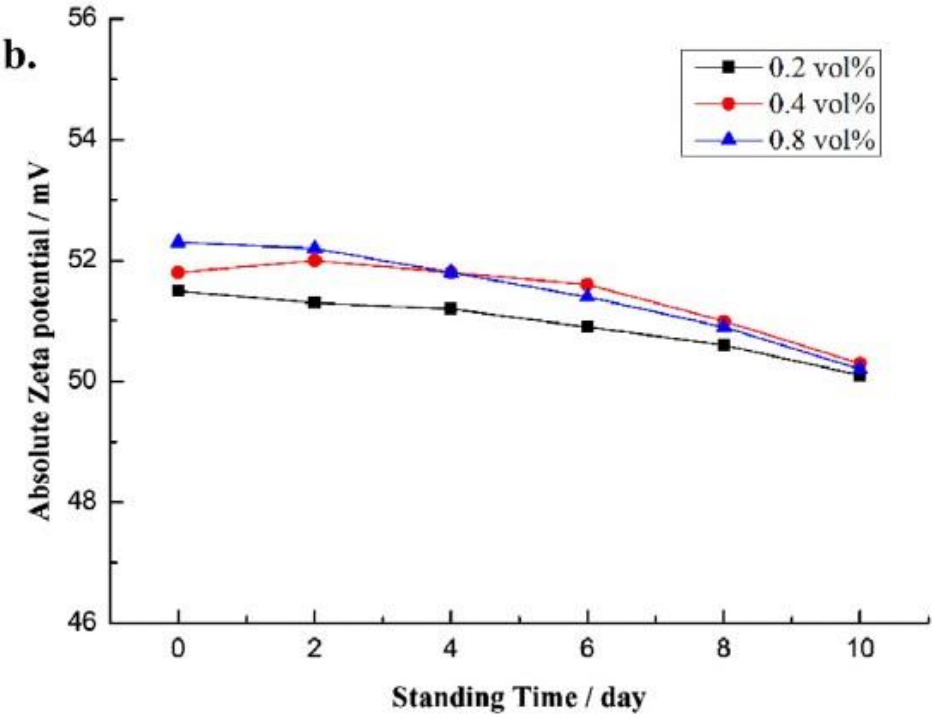


**Fig. 3 Results of the A)sedimentation experiments, and B)zeta potential analysis as a function of time presented by Wei et al.** [56]**. Reprinted with permission from Elsevier with the license number 4542530898908.**

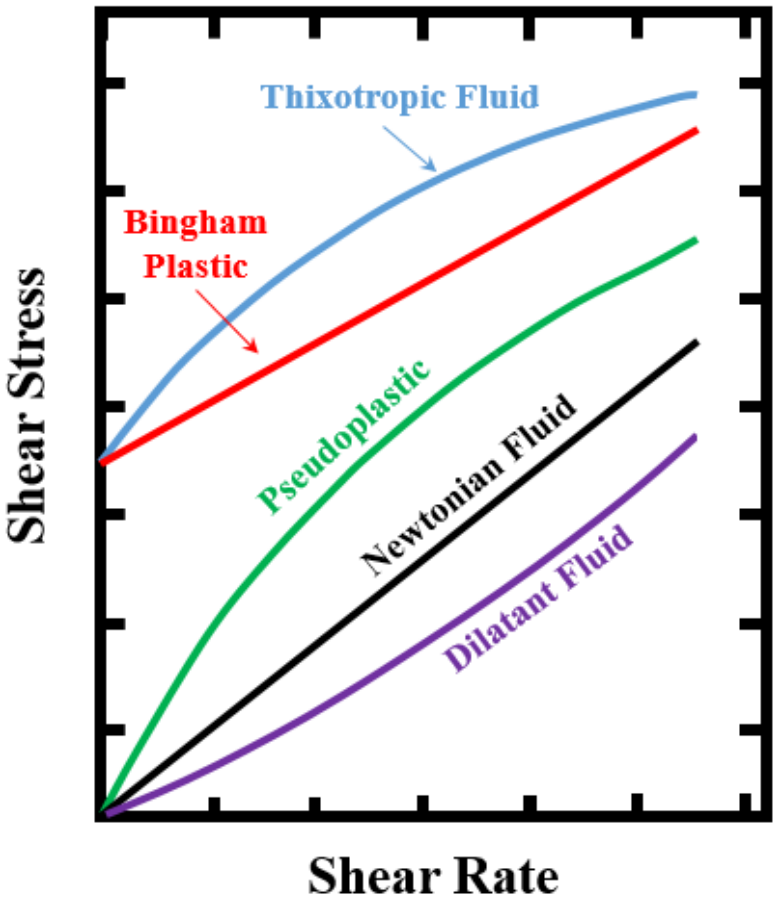


**Fig. 4 The flow behavior of different types of fluids**

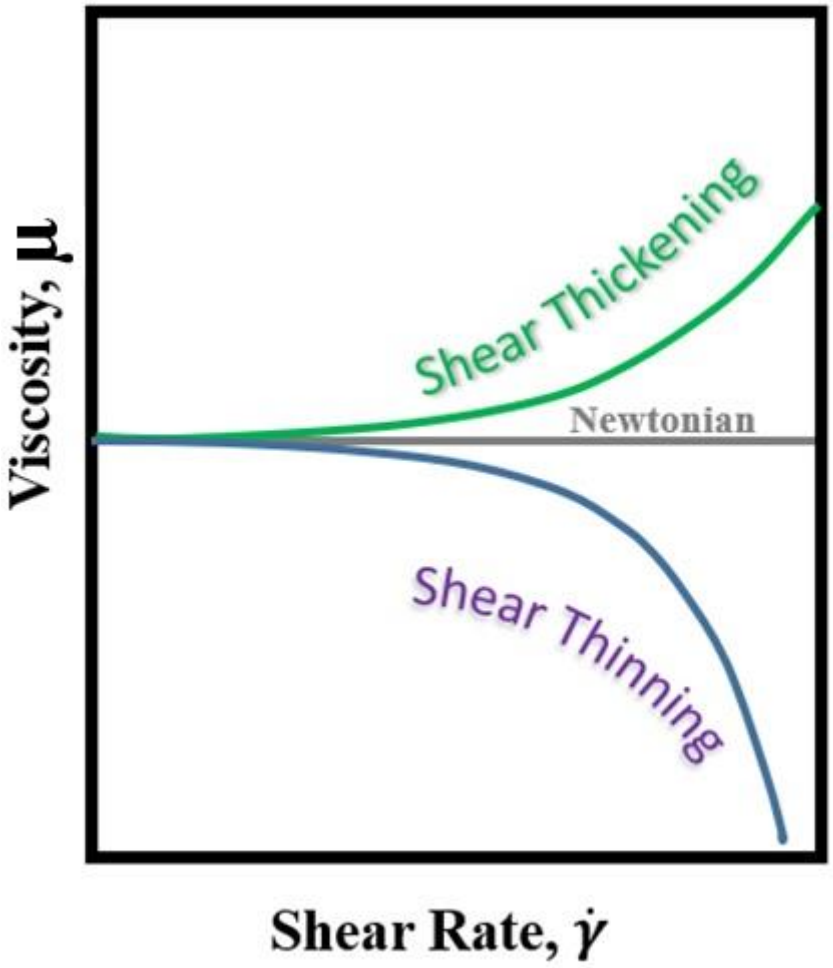


**Fig. 5 Shear thinning and shear thickening behavior**

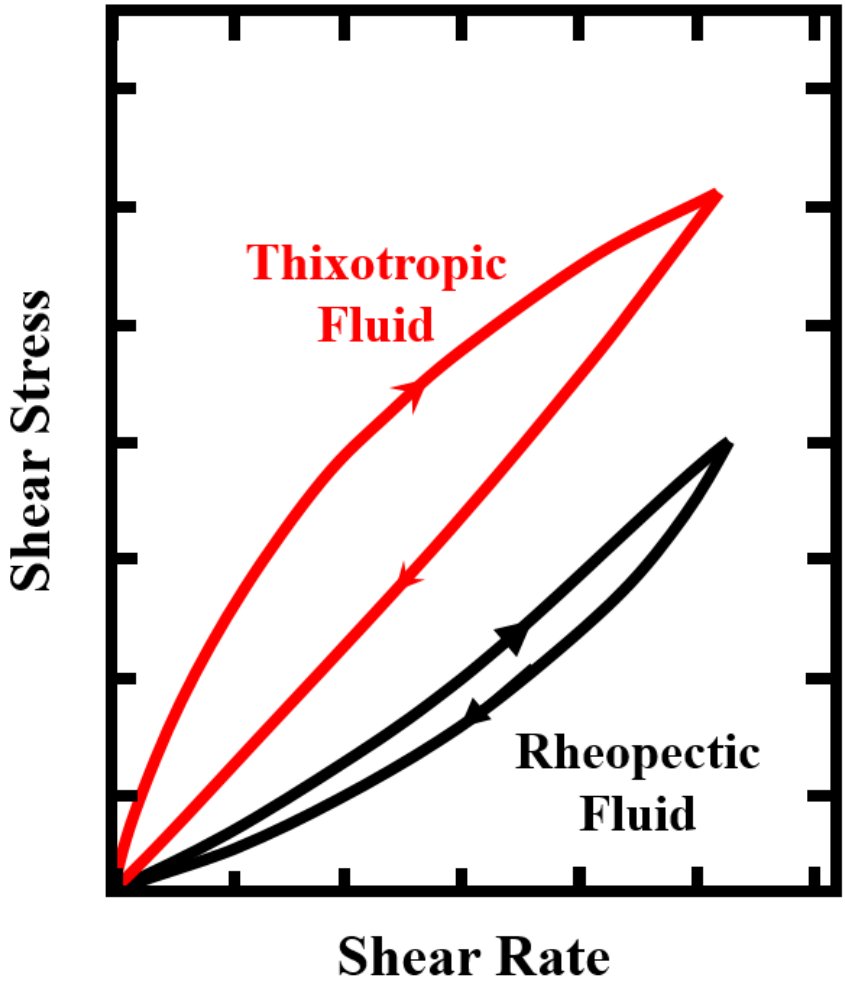


**Fig. 6 The hysteresis loop for time-dependent fluids; Thixotropic and rheopectic fluids**

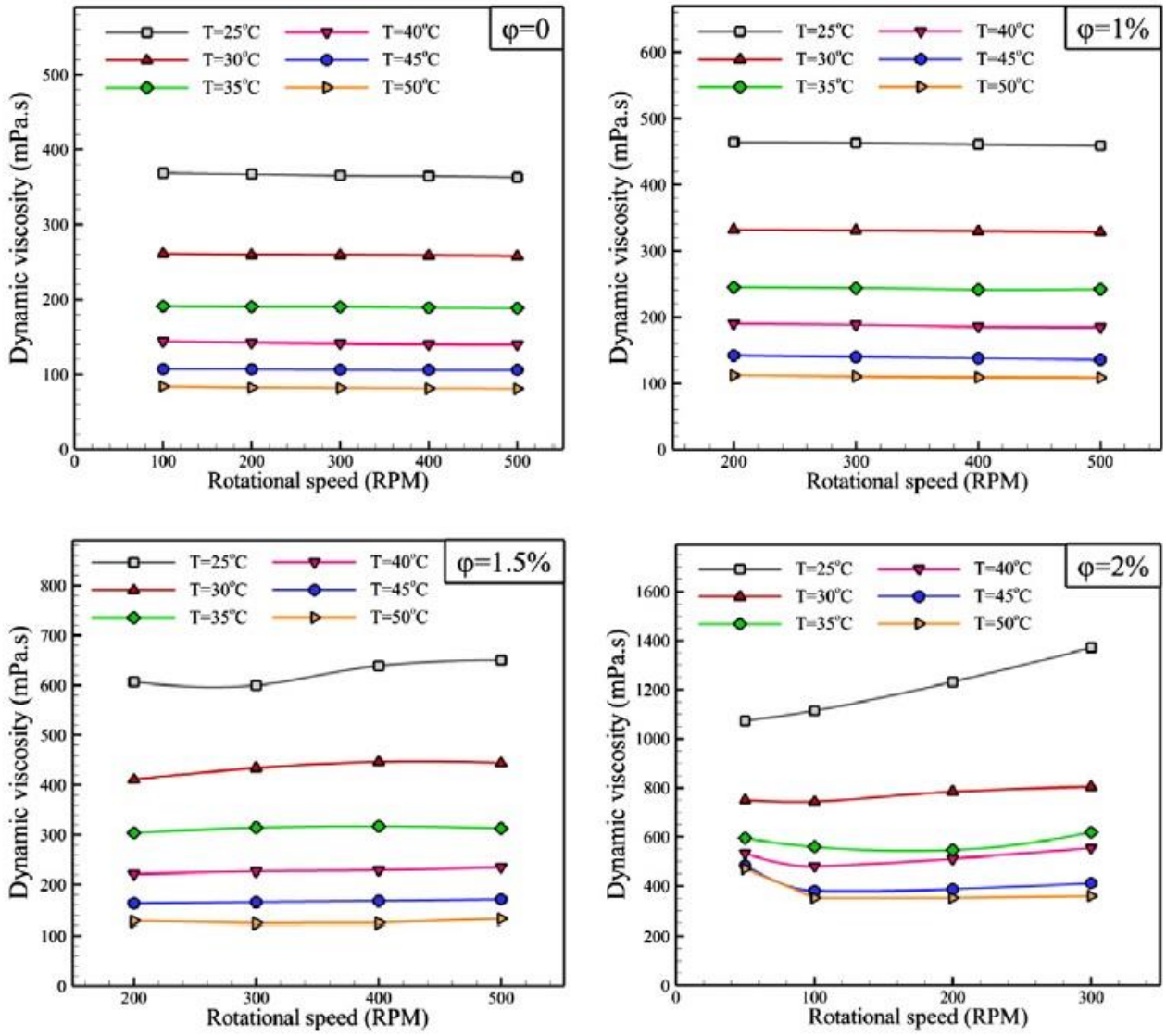


**Fig.7 Newtonian and non-Newtonian behavior of MWCNT-$SiO_2$/oil hybrid NF presented by Hemmat Esfe et al.** [63]**. Reprinted with permission from Elsevier with the license number 4542531118052.**

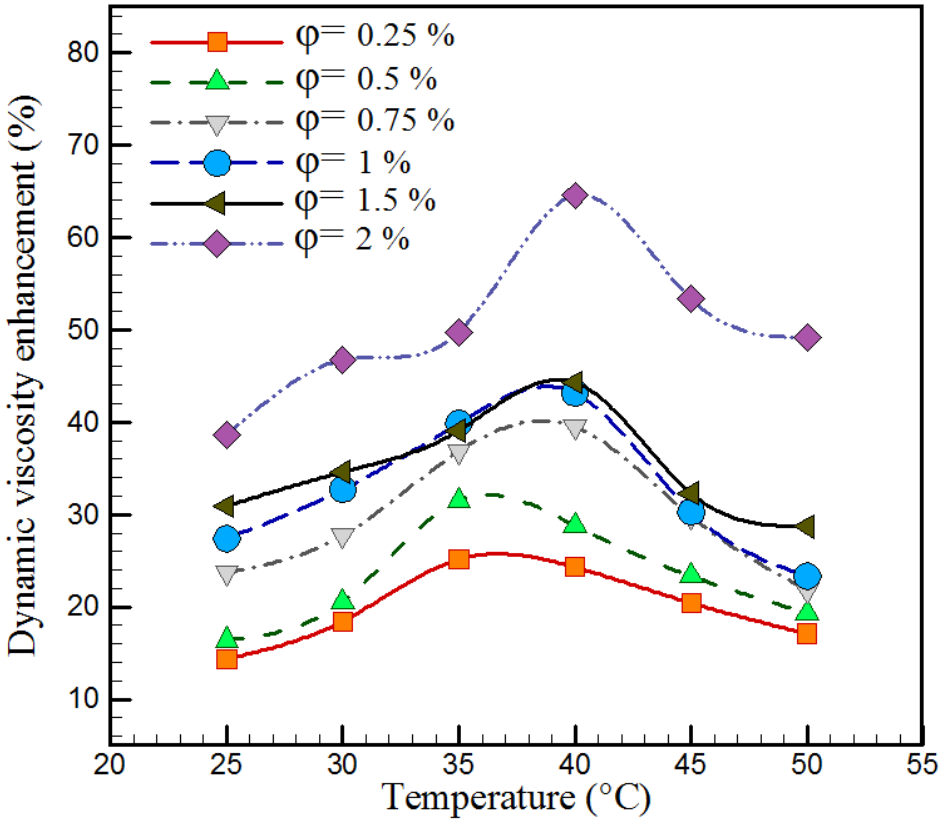


**Fig. 8 Percentage of viscosity increase in different slid concentrations and temperatures presented by Asadi et al.** [61]**. Reprinted with permission from Elsevier with the license number 4542531236569.**

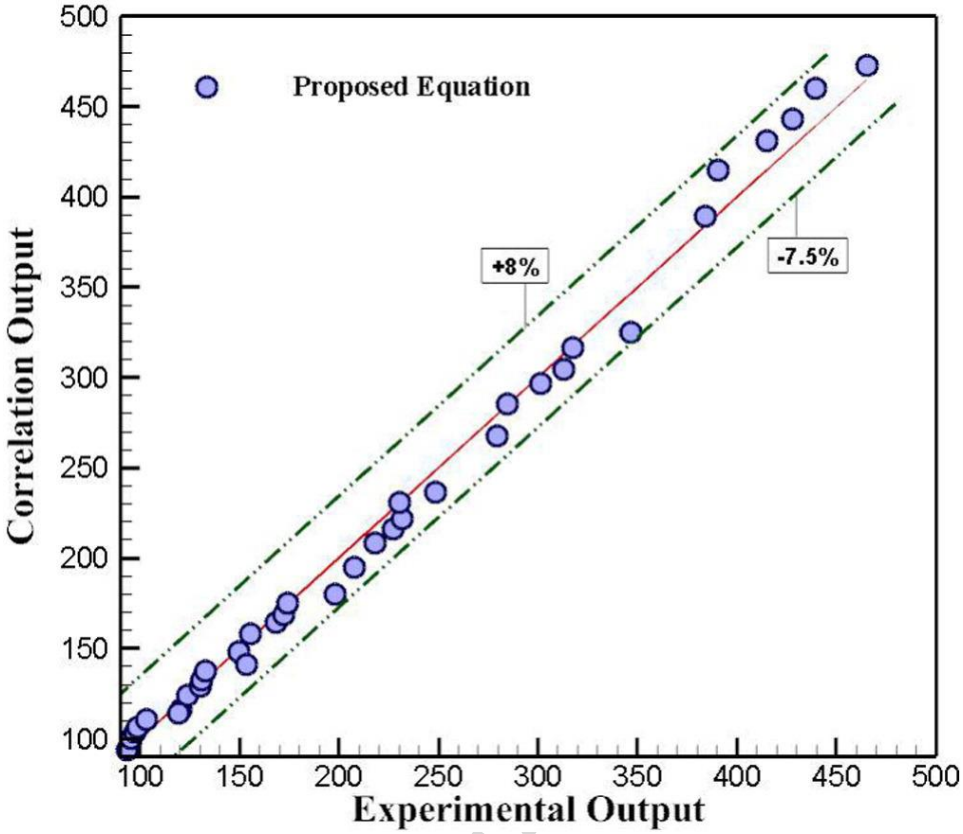


**Fig. 9 Performance of the correlation proposed by Asadi et al.** [61] **to investigate its accuracy in estimating the dynamic viscosity of MgO-MWCNT/engine oil NF. Reprinted with permission from Elsevier with the license number 4542531236569.**

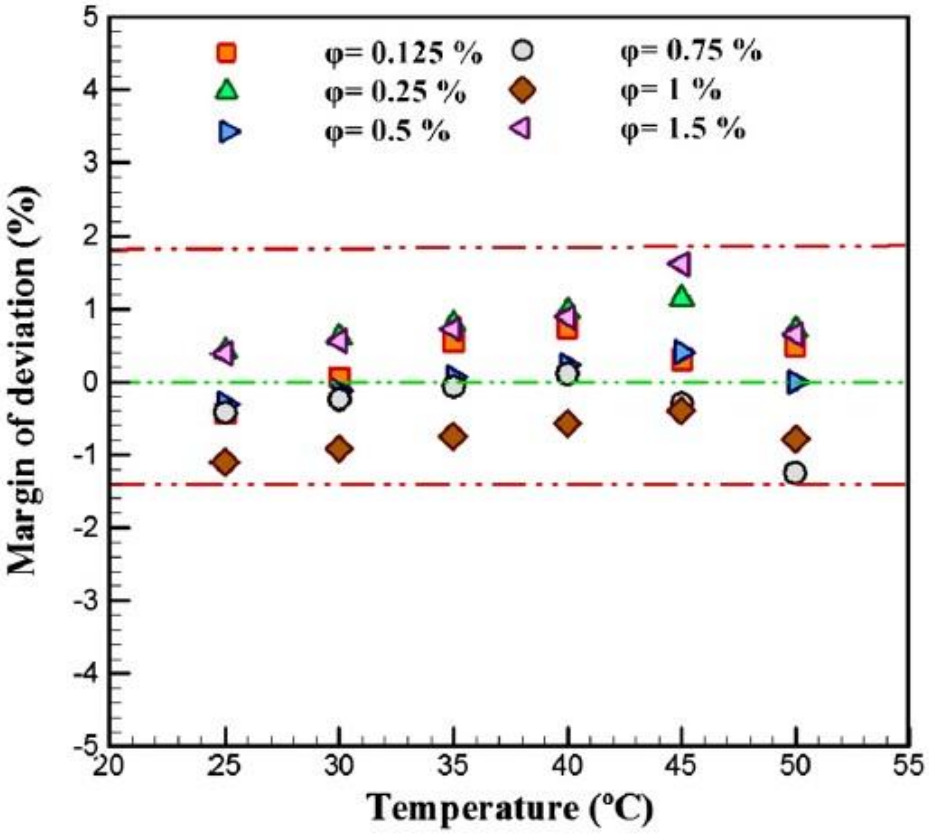


**Fig. 9 Maximum error of the proposed correlation to estimate the thermal conductivity of $Al_2O_3$-MWCNT/oil hybrid NF presented by Asadi et al.** [82]**. Reprinted with permission from Elsevier with the license number 4542531366179.**

**A**

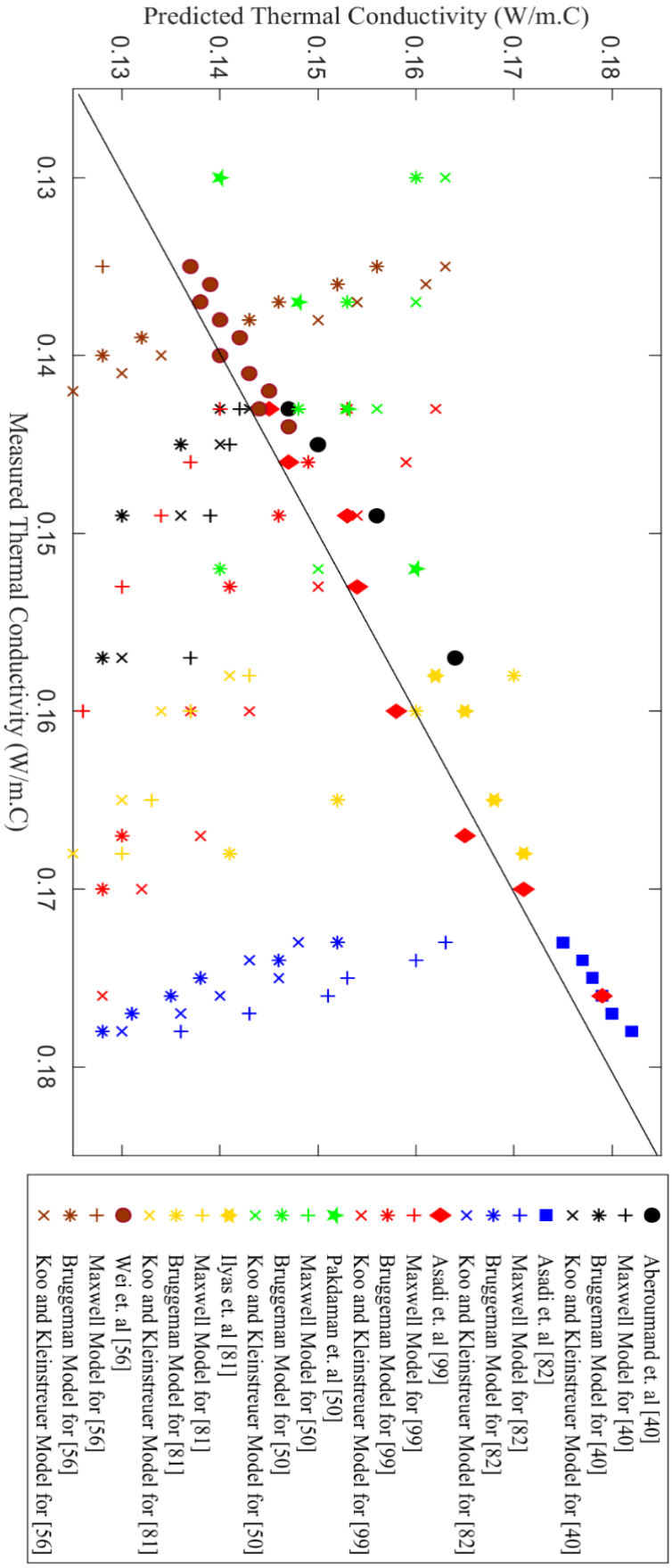

B

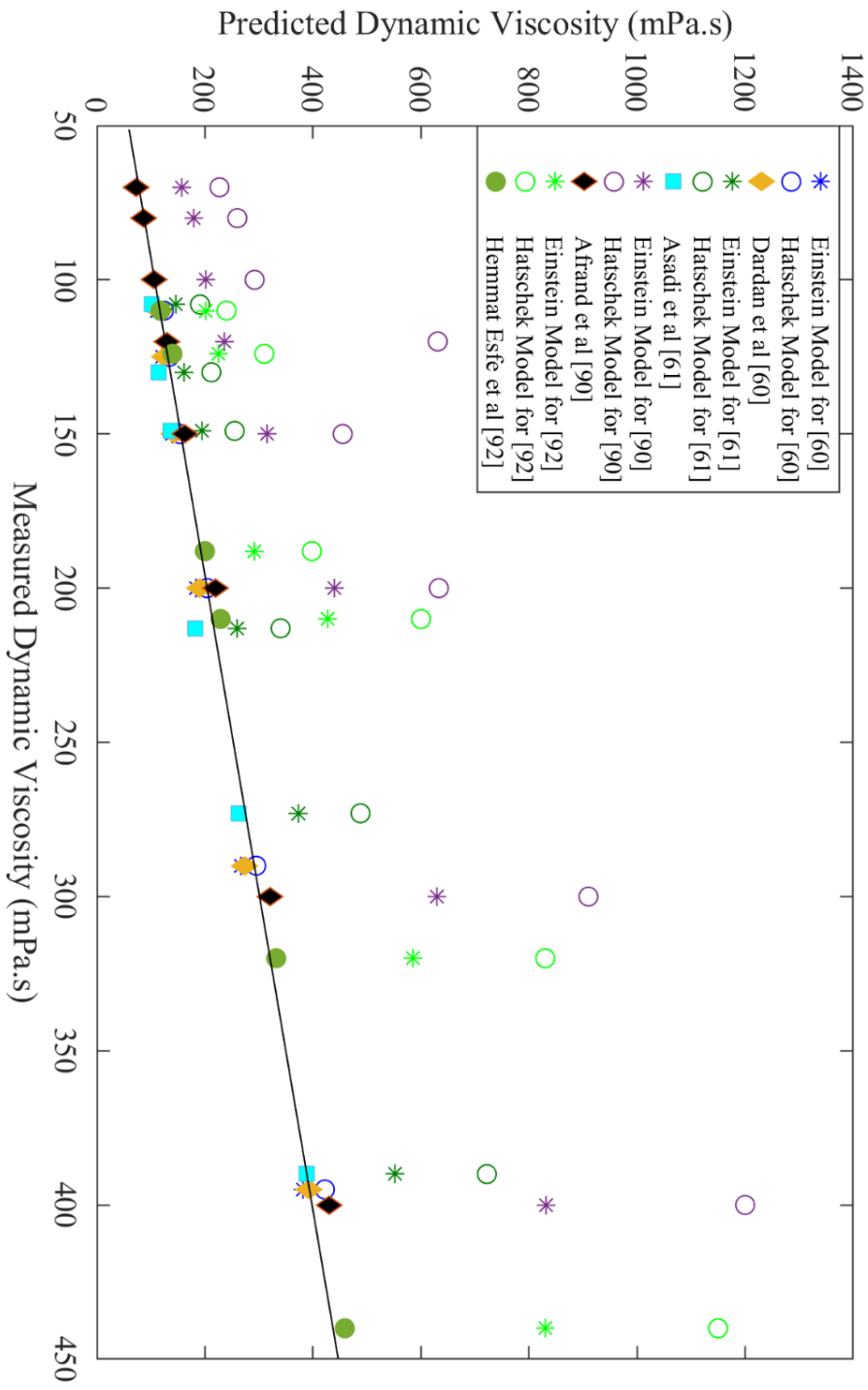


**Fig. 10 Comparison between the proposed experimental models to predict the viscosity and thermal conductivity of different nanofluids with those of the classical models.**

## Tables:

**Table 1 Summary of the preparation methods of oil-based NFs**

| Reference | Nanoparticles | Preparation method |
|---|---|---|
| Aberoumand et al. [40] | Ag | Single-step |
| Botha et al. [88] | Silver-Silica | Single-step |
| Aberoumand and Jafarimoghaddam [41] | Cu | Single-step |
| Farbod et al. [59] | CuO | Single-step |
| Ettefaghi et al. [55] | MWCNT | Two-step |
| Wang et al. [54] | Graphite | Two-step |
| Saeedinia et al. [49] | CuO | Two-step |
| Hemmat Esfe et al. [89] | $Al_2O_3$-MWCNT | Two-step |
| Pakdaman et al. [50] | MWCNT | Two-step |
| Dardan et al. [60] | $Al_2O_3$-MWCNT | Two-step |
| Asadi et al. [61] | MgO-MWCNT | Two-step |
| Hemmat Esfe et al. [63] | $SiO_2$-MWCNT | Two-step |
| Afrand et al. [90] | $SiO_2$-MWCNT | Two-step |
| Li et al. [91] | SiC | Two-step |
| Asadi and Asadi [57] | ZnO-MWCNT | Two-step |
| Hemmat Esfe et al. [92] | ZnO-MWCNT | Two-step |
| Li et al. [93] | SiC-$TiO_2$ | Two-step |
| Asadi and Pourfatah [94] | ZnO and MgO | Two-step |
| Anoop et al. [64] | $Al_2O_3$ | Two-step |
| Colangelo et al. [65] | $Al_2O_3$ | Two-step |
| Ahmadi Nadooshan et al. [95] | $SiO_2$-MWCNT | Two-step |
| Asadi [96] | MWCNT-ZnO | Two-step |
| Hemmat Esfe [97] | ZnO | Two-step |
| Moghaddam and Motahari [98] | CuO-MWCNT | Two-step |

**Table 2 A summary of the studied oil-based NF with Newtonian behavior**

| Reference | Studied nanofluid | Concentrations | Temperatures |
|---|---|---|---|
| Saeedinia et al. [49] | CuO-oil | 0.2-2 wt% | 20-70 ℃ |
| Pakdaman et al. [50] | MWCNT/ oil | 0.1, 0.2, and 0.4 wt % | 40-100 ℃ |
| Farbod et al. [59] | CuO/engine oil (20W50) | 0.2-6 wt % | 5-70 ℃ |
| Dardan et al. [60] | $Al_2O_3$-MWCNT/engine oil (SAE40) | 0.0625 % to 1 % | 25-50 ℃ |
| Hemmat Esfe et al. [63] | MWCNT-$SiO_2$/ engine oil (SAE40) | 0.0625-2 vol.% | 25-50 ℃ |
| Afrand et al. [90] | MWCNT-$SiO_2$/ engine oil (SAE40) | 0-1 vol.% | 25-60 ℃ |
| Li et al. [91] | SiC/diathermic oil | 0.2-0.8 vol.% | 25-60 ℃ |
| Asadi et al. [61] | MWCNT-MgO/ engine oil (SAE50) | 0.25-2 vol. % | 25-50 ℃ |
| Hemmat Esfe et al. [92] | MWCNT-ZnO/ engine oil (SAE40) | 0.05-1 vol. % | 25-60 ℃ |

| | | | |
|---|---|---|---|
| Asadi and Pourfatah [94] | MgO and ZnO/engine oil | 0.125- 1.5 vol. % | 15-55 ℃ |
| Aberoumand et al. [40] | Ag/oil | 0.12, 0.36, and 0.72 wt % | 25 to 60 ℃ |
| Asadi et al. [99] | MWCNT-$Mg(OH)_2$/engine oil | 0.25 to 2 vol. % | 25 to 60 ℃ |
| Li et al. [93] | SiC/waste cooking oil<br>$TiO_2$/waste cooking oil | 0.05 and 1 vol. % | 25-65 ℃ |
| Asadi and Asadi [57] | MWCNT-ZnO/engine oil (10W40) | 0.125-1 vol. % | 5-55 ℃ |
| Wei et al. [56] | SiC-$TiO_2$/diathermic oil | 0-1 vol. % | 25-60 ℃ |
| Asadi et al. [82] | MWCNT-$Al_2O_3$/engine oil | 0.125 to 1.5 vol. % | 25 to 50 ℃ |
| Motahari et al. [100] | MWCNT-$SiO_2$/engine oil (20W50) | 0.05 to 1 vol. % | 40 to 100 ℃ |
| Asadi [96] | MWCNT-ZnO/engine oil | 0.125 to 1 vol. % | 15-55 ℃ |

**Table 3 A summary of the studied oil-based NF with non-Newtonian behavior**

| Reference | Studied nanofluid | Solid concentration | Temperature | Type of the fluid |
|---|---|---|---|---|
| Wang et al. [54] | Graphite/oil | 0.5-4 wt % | 30-60 ℃ | Non-Newtonian, Shear-thinning |
| Hemmat Esfe et al. [63] | MWCNT-$SiO_2$/engine oil (SAE40) | 0.625-2 vol. % | 25 to 50 ℃ | Non-Newtonian |
| Anoop et al. [64] | Alumina/silicon oil | 2-8 wt % | Ambient temperature | Non-Newtonian, Shear-thinning |
| Colangelo et al. [65] | $Al_2O_3$/diathermic oil | 0.3-1 vol. % | 30-50 ℃ | Non-Newtonian |
| Ahmadi Nadooshan et al. [95] | MWCNT-$SiO_2$/engine oil (10W40) | 0.05-1 vol. % | 5-55 ℃ | Non-Newtonian, Shear-thinning |
| Hemmat Esfe et al. [97] | ZnO/engine oil (10W40) | 0.25-2 vol. % | 5-55 ℃ | Non-Newtonian, Shear-thinning |
| Moghaddam and Motahari [98] | MWCNT-CuO/engine oil (SAE40) | 0.0625-1 vol. % | 25-50 ℃ | Non-Newtonian, Shear-thinning |
| Hemmat Esfe et al. [89] | $Al_2O_3$-MWCNT/engine oil (5W50) | 0-1 vol. % | 5-55 ℃ | Non-Newtonian, Shear-thinning |

| | | | | |
|---|---|---|---|---|
| Aberoumand and Jafarimoghaddam [41] | Cu-engine oil | 0.2, 0.5, and 1 wt % | 40-100 ℃ | Non-Newtonian |
| Alirezaei et al. [58] | MWCNT-MgO/engine oil (SAE50) | 0.0625-1 vol. % | 25-50 ℃ | Non-Newtonian |
| Hemmat Esfe et al. [101] | $TiO_2$/engine oil (SAE50) | 0.125-1.5 vol. % | 25-50 ℃ | Non-Newtonian, Shear-thinning |
| Hemmat Esfe et al. [102] | $ZrO_2$-MWCNT/engine oil (10W40) | 0.05-1 vol. % | 5-55 ℃ | Non-Newtonian, Shear-thinning |
| Ilyas et al. [86] | $Al_2O_3$/thermal oil | 0.5-3 wt. % | 25-90 ℃ | Non-Newtonian, Bingham plastic |
| Chai et al. [103] | Graphene nanosheets/hydrogenated oil | 25, 50, and 100 ppm | 30-50 ℃ | Non-Newtonian, Shear-thinning |
| Hemmat Esfe and Esfandeh [104] | MWCNT-MgO/engine oil (SAE40) | 0.25 to 2 vol. % | 25 to 45 ℃ | Non-Newtonian, Shear-thinning |

**Table 4 A summary of the published literature of the dynamic viscosity of oil-based NFs**

| Reference | Nanofluid | Solid concentration | Temperature | Remarks |
|---|---|---|---|---|
| Saeedinia et al. [49] | CuO/oil | 0.2 to 2 wt. % | 20 to 70 ℃ | Minimum viscosity increase of 20 % @ T=20 ℃ |
| Pakdaman et al. [50] | MWCNT/oil | 0.1, 0.2, and 0.4 wt. % | 40 to 100 ℃ | Maximum viscosity increase of 67 % @ T=40 ℃ and φ=0.4 wt. % |
| Ettefaghi et al. [55] | MWCNT/oil (20W50) | 0.1, 0.2, and 0.5 wt. % | 40 to 100 ℃ | Maximum viscosity increase of 1.7 % @ T=40 ℃ and φ=0.5 wt, Maximum viscosity decrease of 0.25 % @ T=100℃ and φ=0.1 wt |
| Farbod et al. [59] | CuO-oil (20W50) | 0.2 to 6 wt. % | 10 to 70 ℃ | - |
| Dardan et al. [60] | $Al_2O_3$-MWCNT/engine oil (SAE40) | 0 to 1 vol. % | 25 to 50 ℃ | Maximum viscosity increase of 46 % @ T= 35 ℃ and φ=1 vol. % |
| Asadi and Asadi [57] | MWCNT-ZnO/engine oil (10W40) | 0.125 to 1 vol. % | 5 to 55 ℃ | Maximum viscosity increase of 45 % @ T= 55 ℃ and φ=1 vol. % Minimum viscosity increase of 19.5 % @ T= 5 ℃ and φ=0.125 vol. % |
| Hemmat Esfe et al. [63] | MWCNT-$SiO_2$/engine oil (SAE40) | 0.0625 to 2 vol. % | 25 to 50 ℃ | Maximum viscosity increase of 1.7 % @ T= 40 ℃ and φ=0.5 wt. % |
| Afrand et al. [90] | MWCNT-$SiO_2$/engine oil (SAE40) | 0 to 1 vol. % | 25 to 60 ℃ | Maximum viscosity increase of 37.4 % @ T= 60 ℃ and φ=1 vol. % |
| Aberoumand et | Ag-oil | 0.12, 0.36, and | 25 to 60 ℃ | Maximum viscosity increase of 41 |

| | | | | |
|---|---|---|---|---|
| al. [40] | | 0.72 wt. % | | % @ T= 25 ℃ and φ=0.72 wt. % |
| Asadi et al. [61] | MWCNT-MgO/engine oil (SAE50) | 0.25 to 2 vol. % | 25 to 50 ℃ | Maximum viscosity increase of 65 % @ T= 40 ℃ and φ=2 vol. % Minimum viscosity increase of 14.4 % @ T= 25 ℃ and φ=0.25 vol. % |
| Hemmat Esfe et al. [92] | MWCNT-ZnO/engine oil (SAE40) | 0.05 to 1 vol. % | 25 to 60 ℃ | Maximum viscosity increase of 33.3 % @ T= 40 ℃ and φ=1 vol. % |
| Colangelo et al. [65] | $Al_2O_3$/diathermic oil | 0.3, 0.7, and 1 vol. % | 30, 40, and 50 ℃ | The effect of adding surfactant on rheological behavior has been studied and found that the viscosity increase is not noticeable in the samples containing Oleic Acid surfactant. |
| Asadi and Pourfatah [94] | MgO and ZnO/engine oil | 0.125 to 1 vol. % | 5 to 55 ℃ | Maximum viscosity increase of 124.3 % for ZnO and 75 % for MgO @ T= 55 ℃ and φ=1.5 vol. %. |
| Ahmadi Nadooshan et al. [95] | MWCNT-$SiO_2$/engine oil (10W40) | 0.05 to 1 vol. % | 5 to 55 ℃ | They reported that increasing the temperature leads to decreasing the consistency factor and power law coefficient. |
| Hemmat Esfe et al. [97] | ZnO/engine oil (10W40) | 0.25 to 2 vol. % | 5 to 55 ℃ | The viscosity at higher temperatures is more sensitive to solid concentration increase. |
| Hemmat Esfe et al. [89] | $Al_2O_3$-MWCNT/engine oil (5W50) | 0.05 to 1 vol. % | 5 to 55 ℃ | The solid concentration increase leads to aggravating the non-Newtonian behavior while increasing the temperature showed the revers effect. |
| Moghaddam and Motahari [98] | MWCNT-CuO/engine oil (SAE40) | 0.0625 to 1 vol. % | 25 to 50 ℃ | Maximum viscosity increase of 29.47 % @ T= 30 ℃ and φ=1 vol. % |
| Aberoumand and Jafarimoghaddam [41] | Cu/engine oil | 0.2, 0.5, and 1 wt. % | 40 to 100 ℃ | Maximum viscosity increase of 37 % @ T= 40 ℃ and φ=1 wt. % |
| Alirezaei et al. [58] | MWCNT-MgO/engine oil | 0.0625 to 1 vol. % | 25 to 50 ℃ | Increasing the temperature from 25 to 50 ℃ leads to 75 % decrease in the dynamic viscosity. |
| Hemmat Esfe and Rostamian [101] | $TiO_2$/engine oil (SAE50) | 0.125 to 1.5 vol. % | 25 to 50 ℃ | The sensitivity analysis showed that the maximum sensitivity was occurred at the solid concertation of 1 vol. % and temperature of 25 ℃. |
| Hemmat Esfe et al. [102] | MWCNT-$ZrO_2$/engine oil (10W40) | 0.05 to 1 vol. % | 5 to 55 ℃ | The maximum increase in the dynamic viscosity was at the temperature of 55 ℃ and solid concentration of 1 vol. % by 31 %. |
| Ilyas et al. [86] | $Al_2O_3$/mineral oil | 0.5 to 3 wt. % | 25 to 90 ℃ | The effect of solid concentration on the dynamic viscosity is negligible at high shear rates. |
| Chai et al. [103] | Graphene | 25 to 100 ppm | 30 to 50 ℃ | Maximum viscosity increase of 33 |

| | | | | |
|---|---|---|---|---|
| | nanosheets/hydrogenated oil | | | % has been reported at the temperature of 30 ℃. |
| Attari et al. [105] | Different oxide NPs ($TiO_2$, NiO, $Fe_2O_3$, ZnO, and $Wo_3$)/crude oil | 0.2 to 2 wt. % | 40 to 100 ℃ | The NPs which possess higher density leads to considerable increase in the dynamic viscosity of the NFs. Moreover, at higher temperatures, the relative viscosity is less than unity. |
| Ilyas et al. [81] | MWCNT/oil | 0 to 1 wt. % | 25 to 90 ℃ | Non-linear decrease of the viscosity by increasing the temperature has been reported. |
| Wei et al. [56] | SiC-TiO2/diathermic oil | 0 to 1 vol. % | 25 to 60 ℃ | They reported increasing trend in the dynamic viscosity by increasing the solid concentration and decreasing trend by increasing the temperature. |
| Li et al. [93] | SiC and $TiO_2$/waste cooking oil | 0.05 and 0.1 vol. % | 25 to 65 ℃ | Both the studied NF showed lower viscosity compared to the BF. |
| Asadi et al. [82] | MWCNT-$Al_2O_3$/oil | 0.125 to 1.5 vol. % | 25 to 50 ℃ | Maximum viscosity increase of 81 % @ T= 40 ℃ and φ=1.5 vol. % Minimum viscosity increase of less than 10 % @ T= 50 ℃ and φ=0.125 vol. % |
| Hemmat Esfe and Esfandeh [104] | MWCNT-MgO/engine oil (SAE40) | 0.25 to 2 vol. % | 25 to 45 ℃ | The results showed that adding MWCNT to the BF considerably increases the dynamic viscosity. |
| Asadi et al. [99] | MWCNT-$Mg(OH)_2$/engine oil | 0.25 to 2 vol. % | 25 to 60 ℃ | Maximum viscosity increase of 50 % @ T= 60 ℃ and φ=2 vol. % Minimum viscosity increase of 5 % @ T= 25 ℃ and φ=0.25 vol. % |
| Motahari et al. [100] | MWCNT-$SiO_2$/engine oil (20W50) | 0.05 to 1 vol. % | 40 to 100 ℃ | Maximum viscosity increase of 171 % @ T= 100 ℃ and φ=1 vol. % |

**Table 5 A summary of the classical model to predict the viscosity of different suspensions**

| Reference | Model | Remarks |
|---|---|---|
| Einstein [66] | $\mu_{eff} = \mu_{bf}(1+2.5\varphi)$ | Suitable for the suspensions with spherical particles in the concentrations less than 1 % |
| Hatschek [106] | $\mu_{eff} = \mu_{bf}(1+4.5\varphi)$ | The model is appropriate to predict |

| | | |
|---|---|---|
| | | the viscosity of two-phase suspensions. |
| Krieger and Dougherty [69] | $\mu_{eff} = \mu_{bf}\left(1-\frac{\varphi}{\varphi_m}\right)^{-2.5}$ | The model is capable of predicting the viscosity of suspensions containing rigid spheres and all the concentrations. |
| Brinkman [67] | $\mu_{eff} = \mu_{bf}(1-\varphi)^{-2.5}$ | Applicable for diluted suspensions of particles. |
| Brenner and Condiff [107] | $\mu_{eff} = \mu_{bf}(1+\eta\varphi)$ where; $\eta = \frac{0.312r}{\ln 2r - 1.5} + 2 - \frac{0.5}{\ln 2r - 1.5} - \frac{1.872}{r}$ | The model considered the shape effect of the rod-like particles at high shear rates for the volume fractions up to $1/r^2$. |
| Jeffrey and Acrivos [108] | $\mu_{eff} = \mu_{bf}\left(3+\frac{4}{3}\left(\frac{\varphi r^2}{\ln\left(\frac{\pi}{\varphi}\right)}\right)\right)$ | The model is proposed to predict the viscosity of non-dilute suspensions containing rod-like particles. |
| Wang et al. [109] | $\mu_{eff} = \mu_{bf}(1+7.3\varphi+123\varphi^2)$ | A model to predict the dynamic viscosity of different NFs. |
| Batchelor [68] | $\mu_{eff} = \mu_{bf}(1+2.5\varphi+6.2\varphi^2)$ | This model takes into account the Brownian motions of particles. |
| Graham [110] | $\mu_{eff} = \mu_{bf}\left((1+2.5\varphi)+\frac{2.25}{\left[1+\left(\frac{h}{2a}\right)\right]}\times\left[\frac{1}{\left(\frac{h}{a}\right)}-\frac{1}{\left[1+\left(\frac{h}{a}\right)\right]}-\frac{1}{\left[1+\left(\frac{h}{a}\right)\right]^2}\right]\right)$ | The model is applicable to the suspensions containing sphere particles. ***h*** and ***a*** represents the inter-particle spacing and the particle radius, respectively. |
| Nielsen [111] | $\mu_{eff} = \mu_{bf}(1+1.5\varphi)e^{\left(\frac{\varphi}{1-\varphi_m}\right)}$ | This power-law model is a generalized |

| | | |
|---|---|---|
| | | equation applicable to the composite materials. |

**Table 6 A summary of the proposed correlation to estimate the viscosity of oil-based NFs**

| Reference | Studied nanofluid | Proposed correlation | Applicability and accuracy |
|---|---|---|---|
| Pakdaman et al. [50] | MWCNT-heat transfer oil | $\frac{\nu_{nf}-\nu_{bf}}{\nu_{bf}}=(-11.23T+5926.5)\varphi^{1.43}$ | At the temperatures of 40 to 100 ℃ and concentrations of 0.1, 0.2, and 0.4 wt. %. $R^2$=0.91 |
| Dardan et al. [60] | $Al_2O_3$-MWCNT/engine oil (SAE40) | $\frac{\mu_{nf}}{\mu_{bf}}=1.123+0.3251\varphi-0.08994T+0.002552T^2-0.00002386T^3+0.9695\left(\frac{T}{\varphi}\right)^{0.01719}$ | At the temperatures of 25 to 50 ℃ and concentrations 0.0625 to 1 vol. %. Maximum error: 2 % |
| Asadi et al. [61] | MgO-MWCNT/engine oil (SAE50) | $\mu_{nf}=328201\times T^{-2.053}\times\varphi^{0.09359}$ | At the temperatures of 25 to 50 ℃ and concentrations of 0.25 to 2 vol. %. Maximum error: Less than 8 % |
| Hemmat Esfe et al. [63] | MWCNT-$SiO_2$/engine oil (SAE40) | $\frac{\mu_{nf}}{\mu_{bf}}=a_0+a_1\varphi+a_2\varphi^2+a_3\varphi^3$ | The values of α would be found in the paper at different temperatures ranging from 25 to 50 ℃ and |

| | | | |
|---|---|---|---|
| | | | concentrations ranging from 0.0625 to 2 vol. %. Maximum error: 1.2 %. |
| Aberoumand et al. [40] | Ag/oil | $\mu_{nf} = \mu_{bf}(1.15 + 1.061\varphi - 0.5442\varphi^2 + 0.1181\varphi^3)$ | At the temperatures ranging from 25 to 60 °C and concentrations of 0.12, 0.36, and 0.72 wt. %. |
| Afrand et al. [90] | MWCNT-$SiO_2$/engine oil (SAE40) | $\frac{\mu_{nf}}{\mu_{bf}} = a_0 + a_1\varphi + a_2\varphi^2 + a_3\varphi^3 + a_4\varphi^4$ | The values of α would be found in the paper at different temperatures ranging from 25 to 60 °C and concentrations ranging from 0.0625 to 1 vol. %. Maximum error: 0.75 %. |
| Hemmat Esfe et al. [92] | MWCNT-ZnO/engine oil (SAE40) | $\frac{\mu_{nf}}{\mu_{bf}} = A + B\varphi + C\varphi^2 + D\varphi^3$ | The values of A, B, C, and D would be found in the paper at different temperatures ranging from 25 to 60 °C and concentrations ranging from 0.05 to 1 vol. %. Maximum error: 2 %. |
| Li et al. [93] | SiC and $TiO_2$/waste | $\frac{\mu_{nf}}{\mu_{bf}} = 0.15 + 2.4\varphi - 0.23\varphi^2$ | At the temperature of 25 °C and |

| | | | |
|---|---|---|---|
| | cooking oil | | concentrations up to 0.1 vol. %. |
| Asadi and Asadi [57] | MWCNT-ZnO/engine oil (10W40) | $\mu_{nf} = 796.8 + 76.26\varphi + 12.88T + 0.7695\varphi T + \frac{(-196.9T - 16.53\varphi T)}{\sqrt{T}}$ | At the temperatures ranging from 5 to 55 °C and concentrations ranging from 0.125 to 2 vol. %. $R^2$=0.9803. |
| Hemmat Esfe et al. [97] | ZnO/engine oil (10W40) | $\frac{\mu_{nf}}{\mu_{bf}} = a_0 + a_1\varphi + a_2\varphi^2 + a_3\varphi Ln(\varphi)$ | The values of α would be found in the paper for the temperatures ranging from 5 to 55 °C and concentrations ranging from 0.25 to 2 vol. %. Maximum error: 1.2 % $R^2$=0.9797. |
| Asadi et al. [82] | MWCNT-$Al_2O_3$/thermal oil | $\mu_{nf} = A + B\varphi$ | The values of A and B would be found in the paper for the temperatures ranging from 25 to 50 °C and concentrations ranging from 0.125 to 1.5 vol. %. Maximum error: less than 5 % |
| Hemmat Esfe et al. [89] | MWCNT-$Al_2O_3$/engine oil (5W50) | $\mu_{nf} = -744.8 + \frac{1806\varphi^{0.01382}}{T^{0.2}}$ | At the temperatures ranging from 5 to 55 °C and concentrations |

| | | | |
|---|---|---|---|
| | | | ranging from 0.05 to 2 vol. %. $R^2$=0.9923. |
| Asadi et al. [99] | MWCNT-$Mg(OH)_2$/thermal oil | $\frac{\mu_{nf}}{\mu_{bf}} = 1604 + 256.8\varphi + 24.73\varphi^3 + 1.615T^2 + 0.07343\varphi T^2 - 83.2T - 7.389\varphi T - 0.01123T^3 - 74.19\varphi^2$ | At the temperatures ranging from 25 to 60 ℃ and concentrations ranging from 0.25 to 2 vol. %. Maximum error: 6.5 %. |
| Moghaddam and Motahari [98] | MWCNT-CuO/engine oil (SAE40) | $\frac{\mu_{nf}}{\mu_{bf}} = a_0 + a_1\varphi\exp(\varphi) + a_2\varphi^2 + a_3\varphi^3$ | The values of α would be found in the paper for the temperatures ranging from 25 to 50 ℃ and concentrations ranging from 0.0625 to 1 vol. %. Maximum error: less than 2 % and $R^2$=0.9803 |
| Alirezaei et al. [58] | MWCNT-MgO/engine oil (SAE50) | $\mu_{nf} = 4\times10^4 + 145\varphi - 240T - 0.061\gamma + 1.9\times10^6\varphi^2 + 0.36T^2$ | At the temperatures ranging from 25 to 50 ℃, concentrations ranging from 0.0625 to 1 vol. %, and shear rates ranging from 670 to 8700 $s^{-1}$. $R^2$=0.98. |
| Hemmat Esfe and Rostamian [101] | $TiO_2$/engine oil (SAE50) | $\frac{\mu_{nf}}{\mu_{bf}} = 1.2854 + 0.1444\varphi - 0.013802T - 0.00175\varphi T$ | At the temperatures ranging from 15 to 55 ℃ and concentrations ranging from 0.125 |

| | | | |
|---|---|---|---|
| | | | to 1.5 vol. %. Maximum error: 1.52 % and $R^2$=0.9751. |
| Hemmat Esfe et al. [102] | MWCNT-$ZrO_2$/engine oil (10W40) | $\frac{\mu_{nf}}{\mu_{bf}} = a_1 + a_2\varphi e^{\varphi} + a_3\varphi^{1.2} + a_4\varphi^3$ | The values of α would be found in the paper for the temperatures ranging from 5 to 55 ℃ and concentrations ranging from 0.05 to 1.5 vol. %. $R^2$=0.9513. |
| Ilyas et al. [86] | $Al_2O_3$/mineral oil | $\mu_{nf} = -1.6752 - \frac{0.7856}{T} + 0.9125(1-\varphi) + 3.4862(1-\varphi)^2 + 134.8479\frac{(1-\varphi)^2}{T^2} - 2.7263(1-\varphi)^3 - 2347.62\frac{(1-\varphi)}{T^3}$ | At the temperatures ranging from 25 to 80 ℃, concentrations ranging from 0.5 to 3 wt. %, and shear rates ranging from 100 to 2000 $s^{-1}$. Mean absolute error: 15 %, and $R^2$=0.9814. |
| Attari et al. [105] | $TiO_2$, $Fe_2O_3$, ZnO, NiO, and $WO_3$/crude oil | $\ln\left[A_1\left(\frac{\mu_{nf}}{\mu_{bf}} + A_2\right)\right] = \left(\frac{\rho_p}{\rho_{bf}}\right)^a + A_3(w)^b\left(\frac{T}{T_0}\right)^c + A_4\left(\frac{T}{T_0}\right)^c$ | The values of the coefficients would be found in the paper for the temperatures ranging from 40 to 100 ℃ and concentrations ranging from 0.2 to 2 wt. %. The maximum error of 20 % and $R^2$=0.96. |

| | | | |
|---|---|---|---|
| Ilyas et al. [81] | MWCNT/thermal oil | $\mu_{nf} = -1.8231 - \frac{0.0686}{T} + 1.7235(1-\varphi) + 3.329(1-\varphi)^2 + 136.7838\frac{(1-\varphi)^2}{T^2} - 3.2363(1-\varphi)^3 - 2347.39\frac{(1-\varphi)}{T^3}$ | At the temperatures ranging from 25 to 90 ℃, concentrations ranging from 0.5 to 3 wt. %, and the shear rate of 100 $s^{-1}$. Average absolute deviation: 4.91 %, and $R^2$=0.97. |
| Li et al. [93] | SiC and $TiO_2$/waste cooking oil | $\frac{\mu_{nf}}{\mu_{bf}} = 0.15 + 2.4\varphi - 0.23\varphi^2$ | At the temperatures ranging from 25 to 65 ℃, and concentrations of 0.5 and 0.1 wt. % |
| Hemmat Esfe and Esfandeh [104] | MWCNT-MgO/engine oil (SAE40) | $\frac{\mu_{nf}}{\mu_{bf}} = 1.10780 - 0.10873\varphi - 1.18666\,\mathrm{E} - 0.003\,\mathrm{T} - 1.76723\,\mathrm{E} - 0.005\gamma + 3.93936\,\mathrm{E} - 0.003\varphi\,\mathrm{T} + 1.14589\,\mathrm{E} - 0.005\varphi\gamma - 1.90857\,\mathrm{E} - 0.007\,\mathrm{T}\,\gamma + 0.037831\varphi^2 + 1.58759E - 0.005T^2 + 2.17677E - 0.009\gamma^2 - 3.83867E - 0.007\varphi\gamma T$ | At the temperatures ranging from 25 to 45 ℃, concentrations ranging from 0.25 to 2 vol. %, and shear rate ranging from 100 to 1000 $s^{-1}$. Maximum error: less than 3 %, and $R^2$=0.9565. |
| Motahari et al. [100] | MWCNT-$SiO_2$/engine oil (20W50) | $\frac{\mu_{nf}}{\mu_{bf}} = 0.09422 - \left[\left(\frac{T}{\varphi}\right)^2 + 0.100556T^{0.8827}\varphi^{0.3148}\right] \exp(72474.75T\varphi^{3.7951})$ | At the temperatures ranging from 40 to 100 ℃, and concentrations ranging from 0.05 to 1 vol. %. Maximum error: less than 5 %, and $R^2$=0.9943 |

**Table 7 A summary of the literature on the thermal conductivity of oil-based nanofluids**

| Reference | Studied nanofluid | Temperature | Solid concentration | Remarks |
|---|---|---|---|---|
| Saeedinia et al. [49] | CuO/oil | 24 to 70 ℃ | 1 and 2 wt. % | in both the concentrations, the thermal conductivity increased as the temperature increased. |
| Wang et al. [54] | Graphite/oil | 30 to 60 ℃ | 0.17 to 1.36 vol. % | Maximum thermal conductivity enhancement of 36 % at the solid concentration of 1.36 vol. % temperature of 60 ℃. |
| Pakdaman et al. [50] | MWCNT/oil | 40 to 70 ℃ | 0.1, 0.2, and 0.4 wt. % | Maximum thermal conductivity enhancement of 15 % at solid concentration of 0.4 wt. % and temperature of 70 ℃. |
| Farbod et al. [59] | CuO/oil | 25 ℃ | 0.2 to 6 wt. % | Maximum thermal conductivity enhancement of 8.3 % at the solid concentration of 6 wt. %. |
| Ettefaghi et al. [55] | MWCNT/engine oil (SAE 20W50) | 20 ℃ | 0.1, 0.2, and 0.5 wt. % | Maximum thermal conductivity enhancement of 22.7 % at solid concentration of 0.5 wt. %. |
| Li et al. [91] | SiC/diathermic oil | 20 to 50 ℃ | 0.2 to 0.8 wt. % | Maximum thermal conductivity enhancement of 7.36 % at solid concentration of 0.8 wt. % and temperature 50 ℃. |
| Aberoumand et al. [40] | Ag/heat transfer oil | 40 to 100 ℃ | 0.12, 0.36, and 0.72 wt. % | The Brownian motion is the responsible mechanism for the thermal conductivity enhancement by increasing the temperature. |
| Colangelo et al. [65] | $Al_2O_3$/diathermic oil | 30 to 50 ℃ | 0.3, 0.7, and 1 vol. % | Adding Oleic Acid surfactant showed no effect on the thermal conductivity enhancement. |
| Aberoumand and Jafarimoghaddam [41] | CuO/engine oil | 40 to 100 ℃ | 0.2, 0.5, and 1 wt. % | The thermal conductivity of the BF showed a decreasing trend by increasing the temperature. The maximum thermal conductivity enhancement is 37 % at the solid |

| | | | | |
|---|---|---|---|---|
| | | | | concentration of 1 wt. % and temperature of 100 ℃. |
| Ilyas et al. [81] | MWCNT/oil | 20 to 60 ℃ | 0.1 to 1 wt. % | The thermal conductivity of the pure oil decreases as the temperature increased. The Brownian motion and thermophoresis are the responsible mechanisms for the thermal conductivity enhancement. The maximum enhancement was 28.7 % at the φ=1 wt. % and T=60 ℃. |
| Ilyas et al. [86] | $Al_2O_3$/oil | 25 to 55 ℃ | 0.5 to 3 wt. % | The thermal conductivity of the pure oil decreases as the temperature increased. The Brownian motion was reported as the main mechanism for thermal conductivity enhancement. |
| Chai et al. [103] | Graphene nanosheets/Hydrogenated oil | 30 to 50 ℃ | 25, 50, and 100 ppm | Maximum thermal conductivity enhancement of 14.4 % at φ= 100 ppm, and T=50 ℃. |
| Asadi [96] | MWCNT-ZnO/engine oil | 15 to 55 ℃ | 0.125 to 1 vol. % | Maximum thermal conductivity enhancement of 40 % at φ= 1 vol. %, and T=55 ℃. |
| Li et al. [93] | SiC and $TiO_2$/waste cooking oil | 30 ℃ | 0.025 to 0.3 vol. % | Adding 3 vol. % dispersant results in 5 % enhancement in the thermal conductivity. |
| Asadi and Pourfatah [94] | MgO and ZnO/engine oil | 15 to 55 ℃ | 0.125 to 1.5 vol. % | Maximum thermal conductivity enhancement of 28 % for ZnO and 32 % for MgO at φ= 1.5 vol. %, and T=55 ℃. |
| Wei et al. [56] | Sic-$TiO_2$/Diathermic oil | 17 to 43 ℃ | 0.1 to 1 wt. % | Maximum thermal conductivity enhancement of 8.39 % at φ= 1 vol. %, and T=43 ℃. |
| Asadi et al. [61] | MWCNT-MgO/engine oil | 25 to 50 ℃ | 0.25 to 2 vol. % | Maximum thermal conductivity enhancement of 62 % at φ=2 vol. %, and T=50 ℃. |
| Asadi et al. [82] | $Al_2O_3$-MWCNT/engine | 25 to 50 ℃ | 0.125 to 1.5 | Maximum thermal conductivity |

| | | | | |
|---|---|---|---|---|
| | oil | | vol. % | enhancement of 45 % at φ=1.5 vol. %, and T=50 ℃. |
| Asadi et al. [99] | MWCNT-$Mg(OH)_2$/engine oil | 25 to 60 ℃ | 0.25 to 2 vol. % | Maximum thermal conductivity enhancement of 50 % at φ=2 vol. %, and T=60 ℃. |

**Table 8 A summary of the proposed empirical-based correlations for estimating the thermal conductivity of the oil-based NFs.**

| Reference | Studied nanofluid | Proposed correlation | Applicability and accuracy |
|---|---|---|---|
| Pakdaman et al. [50] | MWCNT/oil | $\frac{k_{nf}}{k_{bf}} = 1 + 304.47(1+\varphi)^{136.35} \exp(-0.021T)\left(\frac{1}{d_p}\right)^{0.369}\left(\frac{T^{1.2321}}{10^{2.4642B/(T-C)}}\right)$ | The constant B and C are 247.8 and 140, respectively. Applicability: T= 40 to 70 ℃, and φ=0.1 to 0.4 wt. %. Accuracy; Maximum error: 6 %. |
| Aberoumand et al. [40] | Ag/oil | $k_{nf} = (3.6\times10^{-5}T - 0.0305)\varphi^2 + (0.086 - 1.6\times10^{-4}T)\varphi + 3.1\times10^{-4}T + 0.129 - 5.77\times10^{-6}k_p - 40\times10^{-4}$ | Applicability: T= 40 to 100 ℃, and φ=0.12 to 0.72 wt. %. Accuracy: Maximum error: 3.5 %. |
| Ilyas et al. [81] | MWCNT-thermal oil | $k_{nf} = 0.595 - 0.4547(1-\varphi_p) + T\left[0.7422 - 0.606(1-\varphi_p) + \frac{0.2759}{(1-\varphi_p)} - \frac{0.3943}{(1-\varphi_p)^2}\right]$ | Applicability: T= 25 to 63.15 ℃, and φ=0.1 to 1 wt. %. Accuracy: Maximum error: 3.5 %, and $R^2$=0.95 |
| Ilyas et al. [86] | $Al_2O_3$/oil | $k_{nf} = 1.4408 - 0.829(\ln T) + 0.1588(\ln T^2) - 0.0702(1-\varphi_p) - 0.2151(\ln T)(1-\varphi_p) + \frac{0.5965T}{(1-\varphi_p)} - \frac{0.39T}{(1-\varphi_p)^2}$ | Applicability: T= 24.47 to 54.65 ℃, and φ=0.5 to 3 wt. %. Accuracy: Maximum error: ±2 %, and $R^2$=0.96 |

| | | | |
|---|---|---|---|
| Wei et al. [56] | Sic and $TiO_2$/diathermic oil | $k_{nf} = aT^2 + bT + C$ | The constants a, b, and c would be found in the reference. Applicability: T= 17 to 43 ℃, and φ=0.2 to 1 vol. %. |
| Asadi et al. [61] | MWCNT-MgO/engine oil | $k_{nf} = 0.162 + 0.691\varphi + 0.00051T$ | Applicability: T= 25 to 50 ℃, and φ=0.25 to 2 vol. %. Accuracy: Maximum error: 3 %. |
| Asadi et al. [82] | MWCNT-$Al_2O_3$/engine oil | $k_{nf} = 0.1534 + 1.1193\varphi + 0.00026T$ | Applicability: T= 25 to 50 ℃, and φ=0.125 to 1.5 vol. %. Accuracy: Maximum error: 2 %. |
| Asadi et al. [99] | MWCNT-$Mg(OH)_2$/engine oil | $k_{nf} = 0.159 + 1.1112\varphi + 0.003T$ | Applicability: T= 25 to 60 ℃, and φ=0.25 to 2 vol. %. Accuracy: Maximum error: 2 %. |

Graphical abstract